

Light from darkness: history of a hot dark sector

Rupert Coy,^{1,*} Jean Kimus,^{1,†} and Michel H.G. Tytgat^{1,‡}

¹*Service de Physique Théorique, Université Libre de Bruxelles,
Boulevard du Triomphe, CP225, 1050 Brussels, Belgium*

We study a scenario in which the expansion of the early universe is driven by a hot hidden sector (HS) with an initial temperature T' that is significantly higher than that of a visible sector (VS), $T' \gg T$. The latter is assumed to be made of Standard Model (SM) particles and our main focus is on the possibility that dark matter (DM) is part of the hot HS and that its abundance is set by secluded freeze-out. In particular, we study the subsequent evolution and fate of its companion particle after DM freeze-out. To be concrete, we work within a framework in which the DM is a Dirac fermion and its companion a massive dark photon. Coupling between the SM and HS is through kinetic mixing. We provide a comprehensive analytical and numerical analysis, including the subsequent process of thermalization of the two sectors. We use these results to explore the viable parameter space of both the DM matter particle and its companion. Assuming that the DM annihilation cross section is bounded by unitarity, the mass of the DM could be as large as $\sim 10^{11}$ GeV.

I. INTRODUCTION

Despite much experimental and theoretical effort, the nature of dark matter (DM) remains elusive. In recent years, much focus has been put on the possibility that DM is a particle which belongs to a hidden sector (HS). There is no universal definition of a HS, but it is generally understood that its constituents are Standard Model singlets that interact at most feebly with the Standard Model (SM), aka the visible sector (VS) [1]. The dynamics of a HS may be in principle very complex, leading possibly to a rich and fascinating phenomenology, with signatures from colliders to astrophysics and cosmology [2–7]. From a cosmological perspective, it is natural to conceive that a HS and the VS were not in equilibrium with each other during all stages of the evolution of the Universe. In particular, they could have evolved with distinct temperatures, $T' \neq T$. A popular scenario assumes that the HS was initially depleted compared to the VS. In that case, the DM particles and their companions could have been populated through a mechanism called freeze-in [8–12]. Alternatively, the VS could be initially very depleted as at the end of inflation [13]. Indeed, in most inflationary models, the inflaton qualifies as being part of a HS.

In this work, we study a scenario in which the HS was initially more populated than the VS. Specifically, we implement this by assuming that the HS was in thermal equilibrium and was hotter than the VS, $T' \gg T$ [14–17]. This is conceivable if, for instance, the inflaton decayed dominantly into HS particles, a scenario called asymmetric reheating [18–23]. Concretely, we will assume that, at some initial moment, the Universe can be characterised by a temperature ratio such that $\xi_i = T'_i/T_i \gg 1$. We will

also assume that $T'_i \gtrsim m_{\text{dm}}$, with m_{dm} the mass of the DM particle. Since the HS is in thermal equilibrium, the DM abundance is simply determined by thermal freeze-out into lighter HS particles, or DM companion in the sequel, a scenario called secluded freeze-out [24]. Our main objective will then be to follow the subsequent evolution of the companion particles after DM freeze-out. In particular, we want to study how the VS is reheated after DM freeze-out, making sure that the universe is radiation dominated and dominantly made of SM particles by the time of Big Bang Nucleosynthesis (BBN) [25, 26].

To be concrete, we will explore this non-standard cosmological history within dark QED [27, 28] coupled to the SM through kinetic mixing [1, 29]. Dark QED is a very popular model for a HS but it has not yet been studied in the present context, see e.g. [15, 21] for other models. In dark QED, the DM is made of dark electrons and positrons, and their freeze-out occurs through their annihilation into massive dark photons, the DM companion. Due to kinetic mixing, the dark photons are unstable and through their decay they should eventually reheat the VS. Loosely speaking, reheating will refer to the moment at which the VS becomes the dominant form of energy along the expansion of the universe. This may occur in essentially two ways. First, it may happen when the dark photons are still relativistic. We will refer to this as “relativistic reheating”. To our knowledge, this possibility has not been fully addressed in the literature and to study this scenario and its implications is one of our main goals. Alternatively, reheating may take place when the dark photons are non-relativistic, a scenario which, by contrast, we refer to as “non-relativistic reheating”. This case is more familiar and similar situations have been much studied in the literature, starting with the seminal work of Scherrer and Turner [30]. We articulate both scenarios of reheating and in particular we will show that both the onset of heat transfer from the HS to the VS and the final stage of reheating are controlled by what we call the heating parameter, κ , see eq.(6).

*Electronic address: rupertlcoy@gmail.com

†Electronic address: jean.kimus@ulb.be

‡Electronic address: michel.tytgat@ulb.be

While we focus on a specific model, here dark QED, we aim at drawing generic conclusions from our analysis. After putting constraints on the mixing parameter and dark photon mass (see fig.5), we concentrate on the impact of reheating on the DM phenomenology. In particular, we will report our findings in the ξ vs m_{dm} plane, or “domain of thermal dark matter candidates” in the parlance of [31]. A generic upper bound on the DM mass will be set assuming that the DM secluded freeze-out is bounded by unitarity, in the vein of [32]. In particular, we will show, confirming other results, that a secluded DM candidate from a hot HS could be as heavy as $m_{\text{dm}} \lesssim 10^{11}$ GeV, much larger than the standard mass reach for freeze-out of DM particles in equilibrium with the SM sector, see also [14, 15, 17, 33]. Typical evolution patterns for the dark photon and its properties are given in figures 3. Our key findings are summarized in figures 5 for the dark photon and 6 for generic thermal dark matter candidates.

Our work is organised as follows. We establish our groundwork in section II, in which we briefly recap the features of dark QED and write down a set of simple Boltzmann equations that describe the evolution of the hidden and visible sectors, including entropy production. In section III, we give several analytical solutions, studying the evolution of the temperature ratio, $\xi \gg 1$ towards standard cosmological evolution. We identify several possible eras that depend critically on whether reheating occurs in a radiation (relativistic reheating) or matter dominated (non-relativistic reheating) eras. In section IV, we delineate the parameter space of the dark photon in the plane ε vs m' , the dark photon mass, see figure 5. We also briefly consider some possible additional implications of a hot HS, such as the baryon asymmetry of the universe. In section V, we discuss the implications of reheating on DM and present an updated domain of thermal DM candidates, going beyond the specific dark QED model, see figure 6. That section also covers the case of a cold HS ($\xi_i \ll 1$). We finally draw our conclusions. Some appendices cover additional technical details. In appendix A, we give a summary of Maxwell-Boltzmann relations that we use throughout, including for relativistic particles. The problem of entropy production during energy transfer from the HS to VS is revisited in appendix B. Other appendices cover additional technical details.

II. BASIC HS INGREDIENTS

A. Dark QED

We consider a HS that consists of dark QED. DM is made of a Dirac fermion χ (and its anti-particle - we do not consider the possibility of asymmetric dark matter) and the companion is a massive dark photon (γ') [27, 28]. We use primes to denote dark sector quantities, unprimed ones being associated to the VS and the subscript ‘t’ when we refer to their sum. For the purpose of efficient

DM secluded freeze-out, we assume that the dark photon is lighter than the DM, $m' < m_{\text{dm}}$. The DM and dark photons interact with the SM through kinetic mixing [29]. The Lagrangian is

$$\mathcal{L} \supset \bar{\chi}(i\not{D} - m_{\text{dm}})\chi - \frac{1}{4}F'_{\mu\nu}F'^{\mu\nu} + \frac{1}{2}m'^2 A'_\mu A'^\mu - \frac{\varepsilon}{2}B_{\mu\nu}F'^{\mu\nu}, \quad (1)$$

where $B_{\mu\nu}$ is the SM hypercharge field strength. The covariant derivative involves a coupling e' , hence a HS fine structure constant, $\alpha' = e'^2/4\pi$. The dark photons can acquire a mass via the Stueckelberg or the Brout-Englert-Higgs mechanism. We assume that the details of $U(1)'$ symmetry breaking play only a subsidiary role for the fate of the dark photons. The mixing term $B_{\mu\nu}F'^{\mu\nu}$ requires a redefinition of the gauge boson fields in order to write down canonical gauge kinetic terms. There are some subtleties regarding the limit of a massless dark photon, but they play little role in the body our work, see e.g. [34, 35].

B. History of a hot hidden sector in brief

There are several ways to produce DM through kinetic mixing [11, 35, 36]. In these references, it is assumed that the HS is either subdominant or is in thermal equilibrium with the VS. Here, instead, we suppose that the universe was dominated by the HS at early times. We parameterise this by assuming thermal equilibrium in both sectors, characterised by temperatures T' and T . Thus we assume $\xi_i = T'_i/T_i \gtrsim 1$ initially. While dark QED has fewer degrees of freedom than the SM, a large initial ξ generically implies $\rho' \gtrsim \rho$. For $g'_* = 3$ and $g_* = \mathcal{O}(100)$, this requires that $\xi \gtrsim 2.4$.

This section is dedicated to a brief introduction of the stages from $\xi_i \gg 1$ to reheating and then the time of BBN. The details are provided in the subsequent sections but the different stages are shown schematically in fig.1. The initial condition $\xi_i \neq 1$ make sense only if the HS and VS are decoupled. As we shall see, this requires that the kinetic mixing parameter is small enough. Concretely, this will require that $\varepsilon \lesssim 10^{-6}$ at most, see fig.5. The corollary of a small ε is that the dark photons are long-lived. Since the HS is initially much more populated than the VS, we will impose that the dark photons are not too abundant by the time of BBN. This will put a lower bound on ε , also depicted in fig.5.

Next, we will require that the DM abundance is set by annihilation of dark positrons and electrons into dark photons, $\chi\bar{\chi} \leftrightarrow \gamma'\gamma'$, or secluded freeze-out [24]. If $\xi \gtrsim (g_*/g'_*)^{1/3}$ around DM freeze-out, the expansion is dominated by the HS and $H \sim g_*^{1/2}T'^2/m_{\text{pl}}$. Assuming instantaneous freeze-out, the DM relic abundance is then

of the order of

$$Y'_{\text{dm}} = \frac{n_{\text{dm}}}{s'} \sim \frac{x'_{\text{fo}}}{g_*'^{1/2} m_{\text{dm}} m_{\text{Pl}} \langle \sigma v \rangle} \quad (2)$$

where $n_{\text{dm}} = n_{\chi} + n_{\bar{\chi}}$ and $x'_{\text{fo}} = m'/T'_{\text{fo}}$. In this expression, T'_{fo} is the freeze-out temperature and $\langle \sigma v \rangle$ is the thermally averaged DM annihilation cross section into dark photon pairs [13]. The prime on the abundance and entropy is there to emphasise that Y'_{dm} refers to the abundance of DM when the expansion is dominated by the HS. So the entropy is dominantly within the HS. Due to possible entropy production along reheating of the VS, an irreversible process, Y' is general not the final DM abundance.

The DM abundance is Boltzmann suppressed and so $n_{\text{dm}} \ll n_{\gamma'}$ after DM freeze-out. At that moment the HS is dominantly composed of dark photons, $n' \approx n_{\gamma'}$. A self-interacting companion particle, like a non-abelian gauge boson [17] or self-interacting scalar [21], could remain in thermal equilibrium after DM freeze-out, but the dark photons can only interact with DM particles, which are rare after freeze-out. The dark photons are therefore kinetically decoupled and are free streaming after DM freeze-out. As long as the dark photons remain relativistic and dominate the universe, we expect that their distribution is close to the one at equilibrium. We will thus use the temperature T' as a proxy to characterise their abundance, $n' \propto g_*' T'^3$. Initially, the temperature of the dark photons evolves as $T' \propto a^{-1}$. But, through kinetic mixing, they will heat the VS.

The dominant process for this is dark photon decay into pairs of SM particles, with a rate $\langle \Gamma' \rangle \sim (m'/T')\Gamma'$ where m'/T' is due to time dilation. Decays are initially rare but become more and more relevant as time goes by. As we will emphasize, the energy transfer from the HS to the VS is controlled by the following combination of parameters, $\kappa \sim \langle \Gamma' \rangle / H \times (\rho'/\rho)$. We will call the early phase of energy transfer “heating” and κ the “heating parameter”, see eq.6. Simply put, when the heating parameter is $\mathcal{O}(1)$, the energy density transferred from the HS is of the order of the energy density within the VS, $\rho \sim \langle \Gamma' \rangle / H \rho'$ [37]. Thus, if $\kappa \lesssim 1$ at early times, the HS and VS are effectively decoupled and $\xi_i \neq 1$ is a well-defined initial condition. The κ increases as function of the scale factor a . Heating of the VS effectively will begin when the heating parameter becomes $\kappa = \mathcal{O}(1)$. At that moment, the temperature ratio starts to decrease towards $\xi = 1$ but $\kappa = \mathcal{O}(1)$ remains constant, cf fig.1. There are then two possibilities.

First, the temperature ratio can reach $\xi = T'/T = 1$ while the dark photons are still relativistic. Provided that $g_*' \ll g_*$, as is the case for dark QED, most of the energy then lies within the VS, $\rho \gg \rho'$. Adapting a standard nomenclature, we will call this scenario “relativistic heating”. The condition for the moment of reheating is that $\kappa \gtrsim 1$, corresponding essentially to $\langle \Gamma' \rangle \gtrsim H$. As the dark photons are still relativistic, they reach ther-

mal equilibrium with the VS. In general terms, we will call “thermalization” the moment when the dark photons are thermal equilibrium with the VS. In the case of relativistic heating, reheating and thermalization coincide, $T_{\text{rh}} = T_{\text{th}}$. Since $\langle \Gamma' \rangle > H$ after reheating, the dark photons remain in thermal equilibrium with the SM particles. Eventually they become non-relativistic with an abundance that becomes Boltzmann suppressed.

Alternatively, the dark photons may become non-relativistic while the expansion is still dominated by the HS, $\xi \approx m'/T \gtrsim 1$. So the universe becomes matter dominated. The VS keeps being slowly heated by rare dark photon decays until $\Gamma' \sim H$. This stops when most of the dark photons have decayed, $\Gamma'/H \gtrsim 1$, and $\rho > \rho'$. This is the familiar reheating from the decay of a massive particle [30]. We refer to this as non-relativistic reheating, drawing the parallel with the case of relativistic reheating sketched above, see sec.III B. After non-relativistic heating, the abundance of dark photons is suppressed. As a matter of principle, the dark photons can thermalize with the VS if their abundance crosses the γ' equilibrium abundance at temperature T , $n' \sim \exp(-t_{\text{th}}/\tau') \sim n'_{\text{eq}}(T_{\text{th}})$, see [38] and appendix E. Thus, in the case of non-relativistic dark photons, reheating and thermalization are separate events, $T_{\text{th}} \ll T_{\text{rh}}$. Regardless, the abundance of dark photons is negligible after reheating.

In either cases of relativistic or non-relativistic reheating, reheating must occur before BBN, when the universe is both radiation dominated [26, 39] and essentially dominated by the known SM particles [25, 40, 41]. The first condition amounts to requiring that the dark photons decay before BBN; the second requires that they are sufficiently non-relativistic by the time of BBN, or $m' \gtrsim \text{MeV}$, cf. Fig 5. If both conditions are satisfied, then the early universe may have been dominated by a hot HS, $\rho' \gg \rho$. This does not imply that process of reheating of the VS from a HS is without consequences. First, most of the entropy is initially within the HS. Furthermore, extra entropy may be created because the heating of the VS is an irreversible process. While the latter effect may only dilute the DM abundance, eq.(2) both effects can dilute other relics that lie within the VS, like a baryon asymmetry, topological defects, other forms of DM, primordial gravitational waves, etc. Because of its importance, expressions for entropy production are given in the following section and also, re-derived from a different perspective in the appendix B. As we will show, if the baryon asymmetry is created after reheating, the dilution of DM due to entropy production from a hot HS may allow thermal DM to be as heavy as $\sim 10^{11}$ GeV, much heavier than standard bounds, see fig.6 and also [15, 33, 42].

C. Set of simplified Boltzmann equations

We now write down a simplified set of Boltzmann equations (BE) that we will use to track the evolution of the coupled γ' and VS. We begin right after DM freeze-out. The abundance of DM particles is $Y_{\text{dm}} \approx n_{\text{dm}}/s \ll 1$, so DM particles are both decoupled and subdominant. It is thus sufficient to consider equations that involve the γ' and the SM degrees of freedom. Since $\varepsilon \ll 1$, the most important processes are those that occur at lowest order in ε . These are the γ' decay and inverse decay, $\gamma' \leftrightarrow f\bar{f}$, with rate $\Gamma' \propto \varepsilon^2$. Scatterings and annihilation processes, meanwhile, scale as ε^4 , and we have explicitly checked that they are always subdominant. Also, processes like $\gamma' + f \leftrightarrow \gamma + f$, while $\propto \varepsilon^2$, are subdominant initially, since $n \ll n'$. They may play a subsidiary role when ξ approaches 1 and $n \sim n'$, thus potentially accelerating the process of thermalization. For the sake of simplicity, we neglect them.

The BE are obtained by taking moments of the kinetic equations for the particle distributions, $f(\vec{p}, t)$. Since we consider evolution before BBN, the VS is in thermal equilibrium and radiation-dominated (RD), characterised by g_* and T . Somewhat paradoxically, the treatment of the HS is slightly complicated by the fact that after DM freeze-out and before reheating the dark photons are free-streaming. In this work, we make two simplifying assumptions. First, we assume that the HS distribution remains close to equilibrium and so can be characterised by a temperature T' and a chemical potential μ' . Second, we use Maxwell-Boltzmann (MB) statistics, even for relativistic particles. While quantum statistics effects are always relevant for relativistic particles, the errors made using MB instead of Fermi-Dirac or Bose-Einstein statistics are small, $\mathcal{O}(10\%)$ for equilibrium quantities. This is largely compensated by the fact that, say, number densities can be expressed as $n = n_{\text{eq}} \exp(\mu/T)$ with equilibrium quantities given in terms of Bessel functions [43], see appendix A. The parameters T , T' and μ' are determined from the evolution of ρ , ρ' and n' and from these we can also determine the production of entropy, still using MB statistics.

Based on all this, we consider the set of equations

$$\frac{d\rho_t}{dt} + 3(1 + w_t)H\rho_t = 0 \quad (3)$$

$$\frac{dn'}{dt} + 3Hn' = \Gamma' \left(\frac{K_1(x)}{K_2(x)} n'_{\text{eq}}(T) - \frac{K_1(x')}{K_2(x')} n' \right) \quad (4)$$

$$\frac{d\rho'}{dt} + 3(1 + w')H\rho' = m'\Gamma' [n'_{\text{eq}}(T) - n'] , \quad (5)$$

where $x^{(\prime)} = m'/T^{(\prime)}$ and $K_{1,2}$ are modified Bessel functions [43]. The latter implement the temperature dependence of the γ' decay and inverse decay rate, which is Γ' [44] in their rest frame: $\langle \Gamma' \rangle = K_1/K_2 \Gamma'$, with $K_1/K_2 \sim 1/x$ for $x \lesssim 1$, see appendix A.

Eq. (3) expresses the conservation of the total energy

density, $\rho_t = \rho + \rho'$, with $w_t \equiv p_t/\rho_t$ the total equation of the state (EoS) of the fluid, for pressure $p_t = p + p'$. The other two equations capture the evolution of the γ' number density (4) and energy density (5). The latter two are redundant when the dark photons are very non-relativistic, $\rho' \approx m'n'$ and $w' \approx 0$. As stated above, we have assumed that the VS particles are in thermal equilibrium at temperature T , but $n' = n'(T', \mu')$ in general. Hence, while it suffices to track ρ to determine T , in general we must solve for both ρ' and n' . Similar set of equations exist in the literature, albeit with a different focus, see e.g. [45, 46]. Alternatively, we could have written the equations directly for $T^{(\prime)}$ and μ' as in [47]. Finally, it is instructive to directly determine the evolution of the entropies. We do this in appendix B.

III. HS AND VS EVOLUTION

Our story begins right after DM freeze-out ($a_i \geq a_{\text{fo}}$ in fig.1). As the HS consists only of DM and γ' , during freeze-out the DM particles transfer their heat to the dark photons, leading to a relative heating of the HS [47]. The initial temperature ratio we will consider, ξ_i , corresponds to the temperature ratio after DM freeze-out [31]. In the coming sections, we will discuss both analytical solutions and numerical solutions of the BE (3)-(5). This will lead us to identify different characteristic regimes that may occur after DM freeze-out. They are schematically outlined in fig. 1 and partially illustrated by fig. 2. Concrete benchmark cases, corresponding to specific choices of γ' properties, are given in the panels of fig.3.

The VS and HS are assumed to evolve independently early on, in which case T' and T both scale as a^{-1} and the initial temperature ratio is simply a constant. We called this initial condition the ‘plateau’. As we will see, the key condition for the existence of a plateau is that

$$\kappa = \frac{1}{3} \frac{\rho'}{\rho} \frac{\langle \Gamma' \rangle}{H} \lesssim 1 \quad (6)$$

see dashed curves in fig. 2. Assuming a plateau, this parameter increases as $\langle \Gamma' \rangle/H \sim a^3$. As we will see, efficient energy transfer from the HS to the VS or ‘heating’ starts when κ becomes order 1. We therefore call this essential combination of energy densities and rates the ‘heating parameter’; the factor of 1/3 is introduced for convenience. During heating, the temperature ratio starts to decrease, see the solid curves in fig. 2, a solution that turns out to be an attractor.

A. Relativistic reheating

1. Analytical solution

We begin by deriving a simple solution of the BE that will capture the salient features of both the heat-

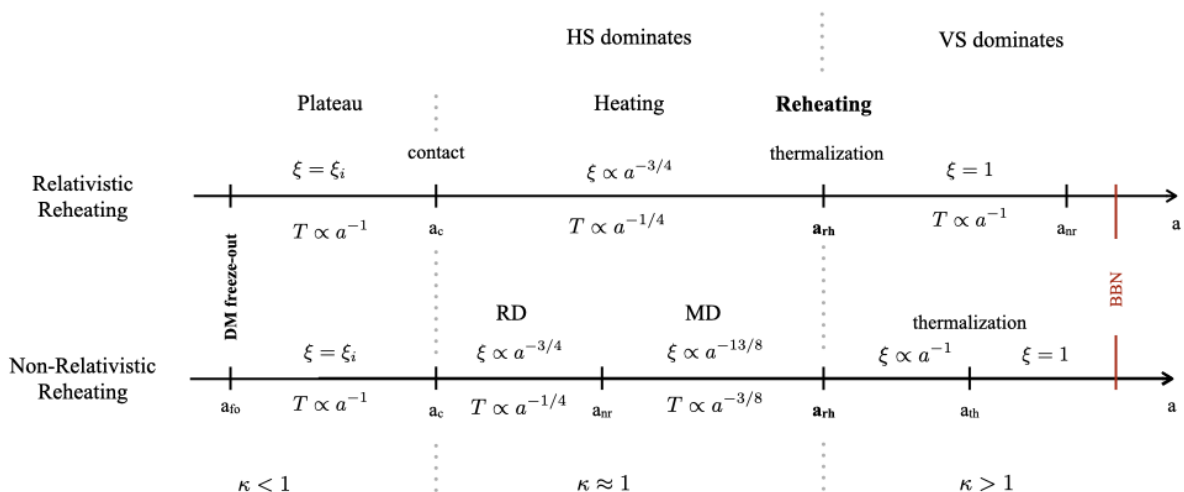


Figure 1: Characteristic evolution of the temperature ratio, $\xi = T'/T \gg 1$, the VS temperature T , and ‘heating parameter’, $\kappa = (\rho'/3\rho) \times \langle \Gamma' \rangle / H$, as functions of the scale factor a , starting from a hot HS with $\xi_i \gg 1$ after the moment of DM freeze-out, a_{fo} . A well-defined scenario requires that the HS is subdominant by the time of BBN. This amounts to requiring that $m' \gtrsim \text{MeV}$. Also, we require that $\kappa \ll 1$ at early times, $\xi \approx \xi_i$ to which we refer as the plateau. Energy transfer, and so ‘heating’ of the VS, effectively starts at moment we call ‘contact’, corresponding to κ reaches 1. The heating parameter remains $\mathcal{O}(1)$ throughout heating and starts to increase after heating is over and the VS is reheated. Relativistic reheating corresponds to parameters such that the dark photons are still relativistic at reheating, thermalize with the VS, with $T' = T$, and remain in thermal equilibrium afterward. Non-relativistic reheating corresponds to scenarios in which the dark photons become NR before the reheating. The dark photons remain out-of-equilibrium, but may thermalize if their abundance reaches the equilibrium one $n'_{eq}(T)$.

ing and thermalization processes. To do so, we assume that the dark photons are relativistic until the moment of thermalization. This suggests assuming that $\mu' = 0$ so that, for instance, the abundance of dark photons can be tracked solely in terms of T' . For reasons that will become clear, this is not entirely appropriate. For the time being, we recall that we use MB statistics, which leads to simple equilibrium relations. Firstly, $w' = 1/3$ for relativistic particles, independent of the chemical potential. Also, $p' = n'T'$ and $\rho' = 3g_*'T'^4/\pi^2$. Finally, $\rho' = \langle E' \rangle n'$ with $\langle E' \rangle = 3T'$. These relations also hold for the VS, for which we also use MB statistics. As usual, it is useful to track evolution in terms of the scale factor a , via $da/dt = aH$. During RD, (3) implies that $\rho_t \propto a^{-4}$ and (5) becomes

$$aH \frac{d}{da} \left(\frac{\rho'}{\rho_t} \right) = \frac{\Gamma'}{3\rho_t} \left[\frac{m'}{T} \rho'_{eq}(T) - \frac{m'}{T'} \rho'(T') \right]. \quad (7)$$

The factors m'/T' and m'/T are caused by time dilation.

Considering Eq. (4), we can write its LHS in terms of ρ' , again using $\rho' = 3n'T'$ and $dT'/dt = -HT'$. On the RHS, $K_1(x')/K_2(x') \equiv \langle m'/E' \rangle \approx x'/2$ for small x' , so that we get the same equation as (7), but with (slightly) more efficient energy transfer rate, $\langle 1/E' \rangle \gtrsim 1/\langle E' \rangle$. The reason for this is simple. The moment $\langle 1/E' \rangle$ is biased towards the low energy part of the γ' distribution, corresponding to the dark photons that decay faster than

the ones with high energy. This implies a departure from equilibrium that, to some extent at least, can be captured through a non-zero chemical potential (we will see this from the numerical solutions in section D). More to the point, it indicates that a fluid approximation is not quite appropriate in the case of relativistic particles. We leave this issue for future work and, sticking to the fluid approximation, we ignore the differences in the definition of the decay rate and use the slightly less efficient rate of eq.(7). As it turns out, our analytical expressions will be both simple and in good agreement with the numerical solutions to the full set of Boltzmann equations.

We make some last simplifications to derive a useful analytical solution to eq.(7). First, we notice that the two terms inside the brackets on the RHS of (7) are of order T^3 and T'^3 respectively. Given that $\xi_i \gg 1$, the dominant term is from decay of the $\gamma' \propto T'^3$, while inverse decay term is not relevant until $T' \sim T$. We therefore set $m'/T \rightarrow m'/T'$ in the first term on the RHS: the numerical difference will be small as long as $\xi \gg 1$, but this change makes the equation easier to handle. Then, using $\rho'_{eq}/\rho_{eq} = (g'_*/g_*)\xi^4$, we can rewrite (7) as an equation for temperatures difference, expressed in terms of

$$\Delta = T'^4 - T^4 \equiv \frac{\pi^2}{3} (\rho'/\bar{g}_* - \rho_t/g_*), \quad (8)$$

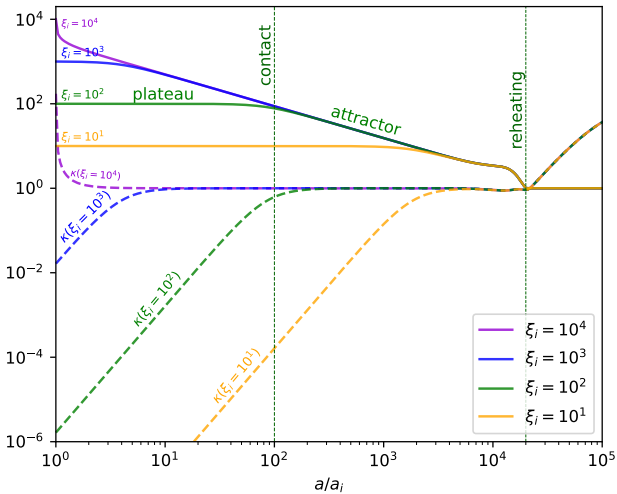


Figure 2: Schematic evolution of the temperature ratio ξ (solid lines) and the heating parameter κ (dashed lines) for different ξ_i ($\varepsilon = 10^{-6}$, $m' = 10$ GeV). This is illustrated for the case of relativistic reheating, meaning that the dark photons are relativistic when ξ reaches 1. The plateau, attractor and the contact times are indicated for the case of $\xi_i = 10^2$. Heating occurs between contact and thermalization. The heating parameter remains constant, $\kappa = \mathcal{O}(1)$, during heating. See text for details and also fig.1. The purple lines (the case of $\xi_i = 10^4$) depict the situation where the temperature ratio is initially unstable (when $\kappa_i \gtrsim 1$).

with $1/\bar{g}_* = 1/g'_* + 1/g_* \approx 1/g'_*$. Thus (7) becomes

$$a \frac{d}{da} \left(\frac{\Delta}{\rho_t} \right) \approx - \frac{g'_*}{\bar{g}_*} \frac{\Gamma'}{3H} \frac{\Delta}{\rho_t} \quad (9)$$

where we have supposed that \bar{g}_* is constant. Since $g_* \gg g'_*$ for most of the parameter space we consider, $g'_*/g_* \approx 1$, so we drop this factor for simplicity.

While the expansion is dominated by the HS, $T' \propto a^{-1}$, so the solution to (9) is

$$\frac{\Delta}{\rho_t} \approx \frac{\Delta}{\rho_t} \Big|_i e^{-(\sigma - \sigma_i)} \quad (10)$$

with $\sigma_i = \langle \Gamma' \rangle_i / H_i = m' \Gamma' / (9T'_i H_i)$ and $\sigma = \sigma_i (a/a_i)^3$. This leads to a simple expression for the evolution of ξ , including thermalization,

$$\xi^4 = \frac{(g'_* + g_* e^{-(\sigma - \sigma_i)}) \xi_i^4 + g_* (1 - e^{-(\sigma - \sigma_i)})}{g'_* (1 - e^{-(\sigma - \sigma_i)}) \xi_i^4 + (g_* + g'_* e^{-(\sigma - \sigma_i)})}. \quad (11)$$

This expression agrees well with our numerical results, see the upper left panel of fig. 3. The black dashed line corresponds to the analytical solution, the green solid curve to the numerical one. There is a small discrepancy between the two curves near $\xi \sim 1$, i.e. thermalization, to which we will return later. From that figure and

Eq (11), we see that the temperature ratio was constant at early times, $\xi \approx \xi_i$, then later evolved towards $\xi = 1$. This initial plateau is necessary for the coherence of our scenario, which rests on the hypothesis that the HS and VS each had well defined temperatures at early times.

2. Heating from relativistic dark photons

Since $\langle \Gamma \rangle / H$ increases in time, heat will eventually start transferring from the HS to the VS. To see the transition of ξ from plateau toward reheating of the VS, we expand the exponential to first order. Assuming $g_* \gg g'_*$ and both $\sigma \ll 1$ and $\xi_i \gg 1$, eq.(11) is well approximated by

$$\xi \approx \frac{\xi_i}{\left(1 + \kappa_i \left((a/a_i)^3 - 1 \right)\right)^{1/4}}. \quad (12)$$

This expression involves the initial value of a combination of parameters that we identify as the heating parameter κ defined in eq.6,

$$\kappa_i = \frac{\rho'_i \langle \Gamma' \rangle_i}{3\rho_i H_i}. \quad (13)$$

While we assumed $\sigma_i \lesssim 1$ to derive (12), κ_i can be smaller or larger than 1, depending on the initial temperature ratio ξ_i . From inspection of (12), we expect that a plateau exists at early times provided $\kappa_i \lesssim 1$. The precise condition turns out to be $\kappa_i < 4/3$, see eq.(22) and section III A 5 where, for completeness, we discuss the case $\kappa_i \gtrsim 1$.

Assuming $\kappa_i \ll 1$, the temperature ratio stays constant while $\kappa = \kappa_i (a/a_i)^3$. It eventually reaches $\kappa \approx 1$, after which ξ starts to decrease, marking the onset of energy transfer from the HS to the VS. We call this event ‘contact’, see fig.2. From (12), contact occurred at

$$\frac{a_{c,i}}{a_i} \simeq \frac{1}{\kappa_i^{1/3}} \sim \left(\frac{g_*}{\sqrt{g'_*}} \frac{T_i'^3}{m' \Gamma' m_{\text{Pl}}} \right)^{1/3} \frac{1}{\xi_i^{4/3}}. \quad (14)$$

Here and below, the subscript i is meant to emphasize the fact that $a_{c,i}$ depends on ξ_i , with contact occurring later for smaller values of ξ_i . From eq.(14), and using that both T and T' evolve as $1/a$ before contact, the temperature of the VS at contact is

$$T_{c,i} \approx 0.4 \left(\frac{g'_*}{g_*} \right)^{1/3} \left(\frac{m' \Gamma' m_{\text{Pl}}}{g_*^{1/2}} \right)^{1/3} \xi_i^{1/3}. \quad (15)$$

Also, for $a \gtrsim a_c$, the temperature ratio evolves as

$$\xi \approx \xi_i \left(\frac{a_{c,i}}{a} \right)^{3/4} \approx \left(\frac{g_*}{g'_* \sigma_i} \right)^{1/4} \left(\frac{a_i}{a} \right)^{3/4}. \quad (16)$$

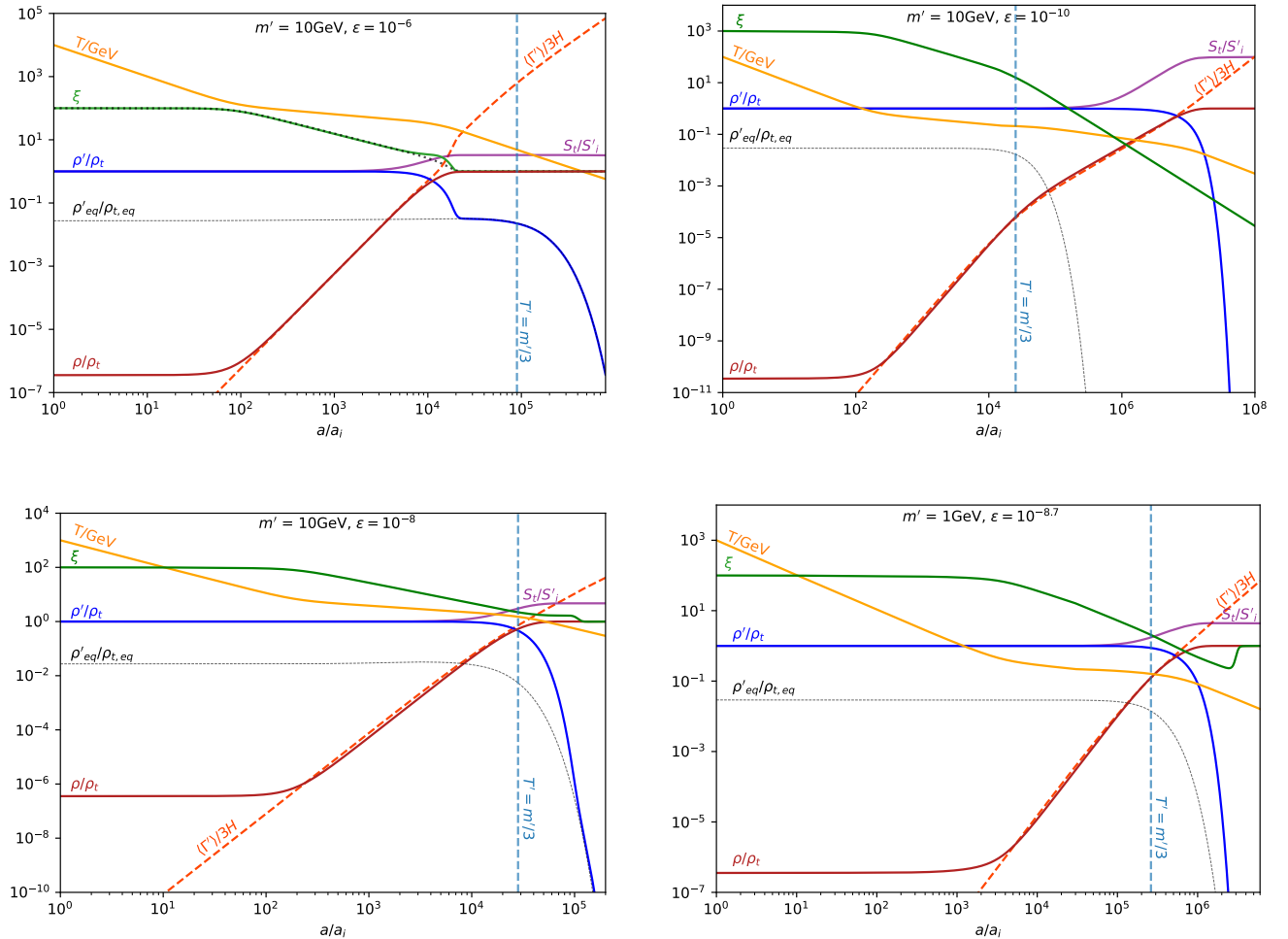


Figure 3: Examples of the different behaviours of the hidden and visible sectors as a function of the scale factor, a . The blue, red and thin grey lines give the ratio of energy densities in each sector, ρ'/ρ_{tot} and ρ/ρ_{tot} , and the ratio $\rho'_{\text{eq}}(T)/\rho_{t,\text{eq}}$ respectively. The green, purple, orange and dashed red lines give the temperature ratio, ξ , the total entropy production, S_t/S'_i , the SM temperature, T/GeV , and the thermally-averaged rate, $\langle \Gamma' \rangle / 3H$, respectively. The dashed vertical blue lines labeled $T' = m'/3$ indicate approximately when the dark photon becomes non-relativistic. The values of m' and ϵ chosen are given in each plot. To avoid unnecessary additional features due to the evolution of g_* in the SM, we have fixed $g_* = 100$ for these figures. The dotted black line in the top-left panel is the analytic expression for ξ , see the comment after eq.(11).

From (14) and (16), we see that ξ is independent of ξ_i after $a_{c,i}$. So this part of its evolution is an attractor, see solid curves in fig.2.

While κ increases before contact, it remains constant during heating, $\kappa \approx 1$, see dashed curves in fig.2. Indeed, from (16), $\rho'/\rho \sim \xi^4 \propto a^{-3}$ while $\langle \Gamma' \rangle / H \propto a^3$. Thus, the energy of the VS evolves as $\rho \approx \rho' \langle \Gamma' \rangle / H$, a behaviour that can be anticipated from Eqs.(3)-(5). For $\xi_i \gg 1$, contact and subsequent heating occur while the decay rate is still (much) less than the Hubble rate, $\langle \Gamma' \rangle / H \ll 1$. For $\xi_i \gg 1$, there is a large reservoir of energy that can transfer from the HS to the VS, hence the relevance of the ratio of rates and energy densities in the heating parameter.

Since $T' \propto a^{-1}$ to a good approximation when $\xi_i \gg 1$,

the temperature of the VS evolves as

$$\frac{T}{T_i} \approx \left(\frac{a_{c,i}}{a} \right)^{1/4} \propto t^{-1/8} \quad \text{and} \quad \xi \propto a^{-3/4}, \quad (17)$$

see e.g. the orange solid curve in the upper left panel of fig.3. The temperature of the VS decreases but quite slowly during heating a behaviour that is qualitatively similar but quantitatively distinct from the case of heating through the decay of a non-relativistic particle, see eq.(33) and the summary of the comparison between relativistic and non-relativistic thermalization in fig.1.

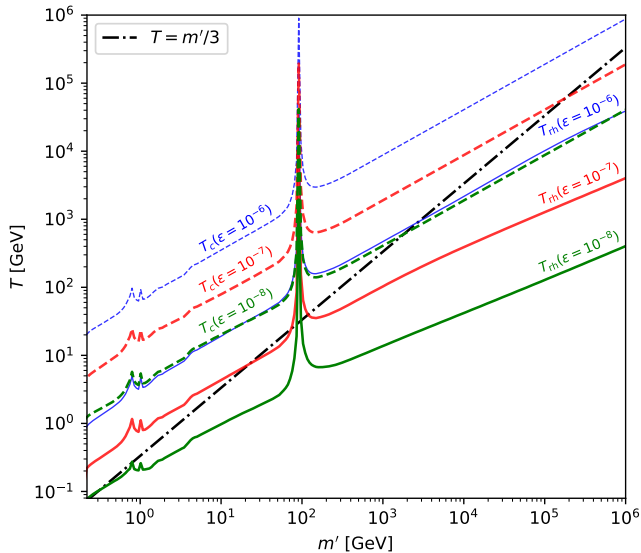


Figure 4: Reheating (solid) and contact (dashed) temperatures in function of m' for different values of ε . Contact temperature is given for $\xi_i = 10^3$. Above (below) the dot-dashed line, the dark photons are relativistic (resp. non-relativistic) at the time of reheating. The features are due to mixing between the γ' and resonances in the SM photon channel, $J/\psi, \dots, Z$. The $\varepsilon = 10^{-6}$ case is the maximal admissible value of the mixing parameter if we take into account the requirement of DM freeze-out in a secluded HS with $\xi_i \gtrsim 1$, as explained in section IV.

3. Thermalization of dark photons and aftermath

According to eq.(11), ξ decreases until the VS and HS reach thermalization. Naively, the condition for this to occur is $\langle \Gamma' \rangle / H \gtrsim 1$. However, numerical solutions (see fig.3) and approximate analytical solution (16) reveal that the reheating condition depends on the relative number of degrees of freedom between the HS and VS. Indeed, $\kappa \approx 1$ at $\xi \approx 1$, corresponding to $\langle \Gamma' \rangle / H \sim g'_*/g_*$, see dashed red curves in fig.3. Once the sectors thermalize, κ increases again, $\kappa \propto \langle \Gamma' \rangle / H$. The heating parameter thus provides a simple criteria to track the energy transfer between the sectors. Put simply, $\kappa < \mathcal{O}(1)$ before heating, ≈ 1 during heating, and $> \mathcal{O}(1)$ after reheating (see Figs. 1 and 2).

Using eq.(16) to estimate the moment of reheating, gives $a_{\text{th}} \approx a_c \xi_i^{4/3}$ and

$$T_{\text{rh}} \approx 0.4 \left(\frac{g'_*}{g_*} \right)^{1/3} \left(\frac{m' \Gamma' m_{\text{Pl}}}{g_*'^{1/2}} \right)^{1/3}. \quad (18)$$

As expected from the attractor behaviour of the evolution of ξ , T_{rh} is independent of ξ_i . Incidentally, (18)

is precisely the same as (15) if we set $\xi = 1$.¹ As expected, T_{rh} is equivalent to the reheating temperature in the more familiar case of decay of a non-relativistic particle, $T_{\text{rh}} \sim \sqrt{\Gamma m_{\text{Pl}} / g_*'^{1/2}}$, see [13] and section IIIB. Indeed, replacing Γ in the latter by the decay rate of a relativistic particle, $\sim (m/T)\Gamma$ gives back (18). The difference is that the HS and VS are made of relativistic degrees of freedom all along.

The entire discussion above assumes that the dark photons are relativistic at T_{rh} . For a given γ' decay rate, the condition that $T_{\text{rh}} \gtrsim m'/3$, together with the expression for the reheating temperature (18), imposes that

$$m' \lesssim \left(\frac{g'_*}{g_*} \right)^{1/2} \left(\frac{m_{\text{Pl}} \Gamma'}{g_*'^{1/2}} \right)^{1/2}. \quad (19)$$

As $\Gamma' \propto \varepsilon^2 m'$, this sets an upper bound on m' for a fixed mixing parameter. Constraints on the mixing parameter and γ' mass will be discussed in section IV. In the meantime, fig.4 illustrates how the reheating (solid) and contact (dashed) temperatures depend on the γ' mass and mixing parameter for $\xi_i = 10^3$ (see also caption). One possible use of this figure may be the following. Consider for instance $\varepsilon = 10^{-7}$ and $m' = 20$ GeV. We see that contact occurred when the temperature of the VS was $T_c \approx 100$ GeV and reheating at $T_{\text{rh}} \approx 6$ GeV, when the γ' was becoming non-relativistic (see dot-dashed line). This implies, that the electroweak phase transition could have occurred along the plateau, with an expansion of the universe driven by a (much) hotter HS [37].

We note that after relativistic reheating, the dark photons remain in thermal equilibrium, even when they become non-relativistic. Unlike annihilation processes, decay and inverse decay processes both remain effective at late time. This is clear for decay, as $\Gamma' > H$ always after reheating. Inverse decay is proportional to the γ' equilibrium abundance, which implies that the γ' always tracks their equilibrium abundance [13, 38], see appendix E. This can be seen in the solid blue curves in fig.3, which depicts the evolution of ρ'/ρ_t . In the upper left panel, corresponding to relativistic reheating, ρ'/ρ_t first drops to $\rho'/\rho_t \approx g'/g_*$ and then becomes Boltzmann suppressed with $\rho' \approx m' n'_{\text{eq}}(T)$ when the dark photons are non-relativistic; the equilibrium abundance at T is depicted as the light dotted curve. The dark photons must thus be heavier than $m' \gtrsim 5$ MeV. Otherwise, their relative abundance is too large to fulfill the ΔN_{eff} condition (see section IV).

The other panels correspond to non-relativistic reheating. In particular, in the lower left panel the dark photons are initially over-abundant when they become NR but

¹ The numerical pre-factor, close to the value 0.34 obtained using (16), has been chosen to closely match the result from the numerical determinations of T_{rh} , as depicted in fig. 4.

eventually track their equilibrium, $\rho' \approx m' n'_{\text{eq}}(T)$. For the choice of parameters depicted in the two right panels, inverse-decay processes are essentially irrelevant and the evolution of the γ' is entirely dominated by direct decay down to very low, and thus negligible, γ' abundances.

4. Relativistic entropy production

The heat transfer from the hidden to the visible sector is an irreversible process, hence entropy production is expected. A direct calculation of entropy evolution is given in appendix B. The outcome is as follows. For relativistic reheating,

$$S_{t,f}/S_{t,i} \approx (g_*/g'_*)^{1/4} \quad (20)$$

where $S_{t,f}$ ($S_{t,i}$) is the final (initial) total comoving entropy. This expression assumes $\rho'_i \gg \rho_i$, so that the initial entropy was dominantly within the HS, $S_{t,i} \approx S'_i$, while $S_{t,f} \approx S_f$ if $g_* \gg g'_*$, see eq.(B22) [31]. In appendix B, we show that the VS entropy increases as $S \propto a^{9/4}$, slightly faster than in the case of non-relativistic decay, $S \propto a^{15/8}$ [30].

For our numerical calculations, entropy is calculated directly from the evolution of the temperatures T and T' using the MB equilibrium expression for the entropy (see appendix A). We checked that our numerical solutions match the asymptotic analytical expressions. An instance of the evolution of the entropy produced in the case of relativistic reheating is depicted by the purple line in the upper left panel of fig.3.

For $g_* \approx 100$ and a massive γ' , the entropy per comoving volume has increased by a factor ~ 3 . After reheating, the DM abundance changed from (2) to

$$Y_{\text{dm}} = \frac{S_{t,i}}{S_{t,f}} Y'_{\text{dm}} \propto \left(\frac{g'_*}{g_*}\right)^{1/4} \frac{x'_{\text{fo}}}{g'^{1/2} m_{\text{dm}} m_{\text{Pl}} \langle \sigma v \rangle}. \quad (21)$$

Entropy dilution in the scenario of relativistic thermalization is modest but non-negligible, being $\mathcal{O}(1)$. It is also irreducible, as an even larger entropy can be produced if the γ' become non-relativistic before thermalization, see section III B.

5. Maximal temperature T_{max}

Before closing the section on relativistic reheating, we comment on the possibility of a large initial heating parameter, $\kappa_i \gtrsim 1$. We have seen that $\kappa_i \lesssim 1$ implies that $\xi \approx \xi_i$, that both the visible and hidden sector temperatures evolve as a^{-1} , and that energy transfer from HS to VS is negligible compared to the amount of energy already present in the VS. A similar condition holds, with exchange $\rho \leftrightarrow \rho'$, if instead the VS is the dominant sector, as in standard freeze-in scenarios. In that case we

must make sure that the Freeze-in contribution does not supersede the initial condition, so that our ξ_i parameter defines well the situation before the start of thermalization. This question is treated in appendix E.

Now consider $\kappa_i \gtrsim 1$. This could correspond to two distinct situations, depending on whether $\langle \Gamma' \rangle / H$ is smaller or larger than 1. The latter would imply that reheating is instantaneous or, i.e. that the HS and VS should immediately be in equilibrium. This contradicts our working hypothesis, so we will use it to put a bound in the kinetic mixing parameter vs. m' mass plane in section IV. The situation in which initially $\langle \Gamma' \rangle / H \lesssim 1$ while $\kappa_i \gtrsim 1$ is more interesting. This corresponds to a very large energy density ratio. Instead of a plateau, the VS temperature first rises to a maximal temperature, $T_{\text{max}} \gtrsim T_{\text{rh}}$. To see this, we employ eq.(12) which, using that $T' \propto a^{-1}$, can be rewritten as

$$\frac{T}{T_i} = \frac{a_i}{a} \left(1 + \kappa_i \left((a/a_i)^3 - 1 \right) \right)^{1/4}. \quad (22)$$

From this, one can check that instead of decreasing, T first rises to reach a maximum T_{max} at

$$\left(\frac{a_{\text{max}}}{a_i} \right)^3 = 4(1 - 1/\kappa_i) > 1. \quad (23)$$

This is provided $\kappa_i > 4/3$, which is the more precise condition for the absence of a plateau. If $\kappa_i \gg 1$, $a_{\text{max}} \approx 2^{2/3} a_i$, so heating to T_{max} is very rapid. As $T' \propto a^{-1}$, for $\kappa_i \gg 1$ this corresponds to

$$T_{\text{max}} \approx \frac{(3\kappa_i)^{1/4}}{4^{1/3}} T_i \approx 0.6 g_*^{-1/4} (\langle \Gamma' \rangle_i m_{\text{Pl}})^{1/4} (g'_* T_i'^4)^{1/8}. \quad (24)$$

The temperature ratio at a_{max} is

$$\xi(a_{\text{max}}) \approx \frac{\xi_i}{(3\kappa_i)^{1/4}} < \xi_i, \quad (25)$$

which is independent of ξ_i since $\kappa_i \propto \xi_i^4$. As T reaches T_{max} , the heating parameter rapidly decreases toward $\kappa \sim 1$ and stays so until reheating (see the dashed purple curve in fig.2).

A rapid increase of the VS temperature is at odds with our basic assumption, namely that the hidden and visible sectors are effectively decoupled around DM freeze-out. Later on, we will use the condition $\kappa_i \lesssim 1$ to set constraints on the possible initial temperature ratio ξ_i in the domain of thermal DM candidates, see sections IV and V.

This is very similar to the standard inflationary scenario. In that case, the HS consists only of the inflaton and the VS is essentially at zero temperature so that reheating to T_{rh} is preceded by a rapid rise to a maximal temperature $T_{\text{max}} > T_{\text{rh}}$ [13, 45]. Eq.(24) can be directly compared with the corresponding expression in the case of inflaton decay with mass M_I , initial abun-

dance $\rho_I \sim M_I$ and decay rate Γ_I ,

$$T_{\max} \approx g_*^{-1/4} (\Gamma_I m_{\text{Pl}})^{1/4} \rho_I^{1/8} \quad (26)$$

see [13, 45]. The equivalence between the two cases amounts to replacing Γ_I by $\langle \Gamma' \rangle_i$ and ρ_I by ρ'_i .

B. Non-relativistic reheating

In the previous section, we considered the possibility that reheating of the VS occurred when the dark photons are still relativistic, $T_{\text{rh}} \gtrsim m'/3$. As expected and as fig. 4 shows, heavier and/or longer-lived dark photons tend to become non-relativistic when the HS is still hotter than the VS, at which point the universe becomes matter-dominated. The key characteristics of this non-relativistic reheating scenario are given in the lower part of fig. 1. Typically, the evolution of the temperature ratio starts with a plateau, followed by an early phase of relativistic heating, until the dark photons become NR. The problem of heating through the decay of a non-relativistic particle is textbook [13, 30]. However, some specific features in our scenario are less standard. In particular, in this section we study the transition from the relativistic to the non-relativistic regime and how this information can be used to determine the entropy dilution factor.

1. Heating from non-relativistic dark photons

We consider dark photons that becomes non-relativistic while $T' \gg T$. Using MB statistics, this occurs roughly when $T' = T'_{\text{nr}} \approx m'/3$. Assuming first a phase of relativistic heating, this corresponds to $a_{\text{nr}} \simeq 3T'_i a_i / m'$ with ξ_{nr} given by (16). At that moment, the dark photon decay rate is still smaller than the expansion rate and, as we will see below, the temperature of the VS evolves as $a^{-3/8}$, see fig. (1). We refer to this regime as non-relativistic heating (or reheating depending on the context) [30].

For non-relativistic dark photons, Eqs.(4) and (5) become essentially equivalent, since $\rho' \approx m' n'$. Neglecting dark photon inverse decays, since the HS dominates, the equations reduce to

$$\frac{dn'}{dt} + 3Hn' \approx -\Gamma' n', \quad (27)$$

with solution

$$n' a^3 = a_{\text{nr}}^3 n'_{\text{nr}} \exp\left(-\frac{2\Gamma'}{3H_{\text{nr}}} \left((a/a_{\text{nr}})^{3/2} - 1\right)\right) \quad (28)$$

using that the expansion is MD, and following the evolution from when the dark photons became non-relativistic.

From Eq. (3), the VS energy density evolves as

$$\frac{d}{da}(\rho a^4) = \frac{m' \Gamma' n' a^3}{H}. \quad (29)$$

The non-relativistic heating period corresponds to the early heating of the VS, when $\Gamma' \lesssim H$, in which case the exponential in (28) is close to 1. In this approximation, integrating (29) gives

$$\rho = \rho_{\text{nr}} \left(\frac{a_{\text{nr}}}{a}\right)^4 + \frac{2}{5} \frac{\Gamma'}{H_{\text{nr}}} \rho'_{\text{nr}} \left(\frac{a_{\text{nr}}}{a}\right)^4 \left(\left(\frac{a}{a_{\text{nr}}}\right)^{5/2} - 1\right) \quad (30)$$

which we can rewrite as an equation for the evolution of T for $\Gamma' \lesssim H$,

$$\frac{T}{T_{\text{nr}}} = \frac{a_{\text{nr}}}{a} \left(1 + \frac{6}{5} \kappa_{\text{nr}} \left((a/a_{\text{nr}})^{5/2} - 1\right)\right)^{1/4} \quad (31)$$

where

$$\kappa_{\text{nr}} = \frac{\rho'_{\text{nr}}}{3\rho_{\text{nr}}} \frac{\Gamma'}{H_{\text{nr}}}. \quad (32)$$

Eq.(31) is the counterpart of (22). The factor $6/5 \approx 1$ is there because the expansion is MD instead of RD and $\langle \Gamma' \rangle = \Gamma'$. Otherwise, the features are the same as for (22). For small $\kappa_i \ll 1$, $\kappa \propto a^{5/2}$, instead of $\propto a^3$ in the case of relativistic dark photon, while $\kappa = \mathcal{O}(1)$ during the early phase of heating, as $\rho \approx \rho' \Gamma' / H$.

Here, we want to track the evolution of T (and ξ) starting with relativistic dark photons, see fig. 1. The heating parameter $\kappa_{\text{nr}} = \mathcal{O}(1)$ when the γ' particles become non-relativistic, and

$$\frac{T}{T_{\text{nr}}} \approx \left(\frac{a_{\text{nr}}}{a}\right)^{3/8} \propto t^{-1/4} \quad (\text{ST}) \quad (33)$$

for $a \gtrsim a_{\text{nr}}$. Since the dark photons are non-relativistic and indeed decoupled, their temperature (or more precisely, mean energy) scales as $T' \propto a^{-2}$, so that $\xi \propto a^{-13/8}$. An instance of such evolution is depicted in the upper right panel of fig. 3, see the green and orange curves for ξ and T . See also $\rho/\rho_t \approx \rho/\rho'$ (solid red) and $\langle \Gamma' \rangle / 3H$ (dashed red) which imply that $\kappa = \rho' / \rho \langle \Gamma' \rangle / 3H \sim 1$ during both the phase of relativistic and non-relativistic heating.

2. Non-relativistic entropy production

From eq.(30), we see that the VS energy density evolves as $\rho \sim \rho' \Gamma' / H$ until $\Gamma' \sim H$, at which point the γ' particles have shed most of their energy into the VS. The entropy produced can be derived from the evolution of the temperature T using the MB relation $s = 4\rho/T$. This implies that the VS comoving entropy evolves as $S \propto a^{15/8}$. Alternatively, we can directly solve a Boltz-

mann equation for entropy evolution [13, 30]. As the situation we consider is non-standard, we revisit this in appendix B. In the present section, we just quote key results.

Considering dark photons that became non-relativistic at a_{nr} , the final entropy after their decay is given by eq.(B11),

$$\frac{S_{t,f}}{S_{t,i}} \approx \frac{S_f}{S_i} \approx \left(\frac{g_*}{g'_*}\right)^{1/4} \left(\frac{\tau'}{t_{\text{nr}}}\right)^{1/2} \quad (34)$$

with $\tau' = 1/\Gamma' \gtrsim t_{\text{nr}}$. The inverse of this factor leads to entropy dilution of the initial DM abundance, as in eq.(21). Eq.(34) stems from the more general expression (B8), assuming $\tau' \gtrsim t_{\text{nr}}$, using MB statistics to relate entropy to energy densities, and using the fact that before the dark photons are non-relativistic, the entropy is dominantly within the HS. We see that the more stable the γ' , the larger is the entropy produced, with a ratio that grows as the square root of the γ' lifetime. If $\tau' \sim t_{\text{nr}}$, we recover the entropy produced in the case of relativistic heating, eq.(B22). We have checked that (34) is in very good agreement with our numerical calculations.

Note that thermalization does not proceed as simply as in the relativistic case (section III A 5). In the NR case, the entropy produced reaches a maximum roughly when $\rho' \approx \rho$ and the expansion is again RD, dominated by the VS. The temperature of the VS at that moment is the standard heating temperature

$$T_{\text{rh}} \sim \left(\frac{m_{\text{Pl}}\Gamma'}{g_*^{1/2}}\right)^{1/2} \quad (35)$$

after which $T \propto a^{-1}$ [13, 30]. The γ' particles are sub-dominant and will keep on decaying. If at some moment $n' \propto e^{-t/\tau'} \sim e^{-m'/T}$, then, due to inverse decay processes, the dark photons will follow an equilibrium abundance at the temperature of the VS, $n' = n_{\text{eq}}(T)$, see [38] and appendix E. We refer to this as the equivalent of thermalization in the non-relativistic scenario, see fig.1. An instance of such evolution is depicted in the lower right panel of fig.3. Note that T' , which was decreasing as a^{-2} characteristic of NR particles, rises toward T after thermalization occurs. In the top right panel, we depict a case for which thermalization never takes place in practice, in the sense that inverse decay processes are negligible down to extremely low γ' number densities. This is evident from the difference between the blue ‘true’ and dashed grey ‘equilibrium’ ratios for ρ'/ρ_t .

IV. DOMAIN OF HOT DARK PHOTONS

We now use the results from the previous sections to delineate a domain in the $\varepsilon - m'$ parameter space consistent with our scenario, see fig. 5. The implications for the Domain of the DM particle χ are discussed in the

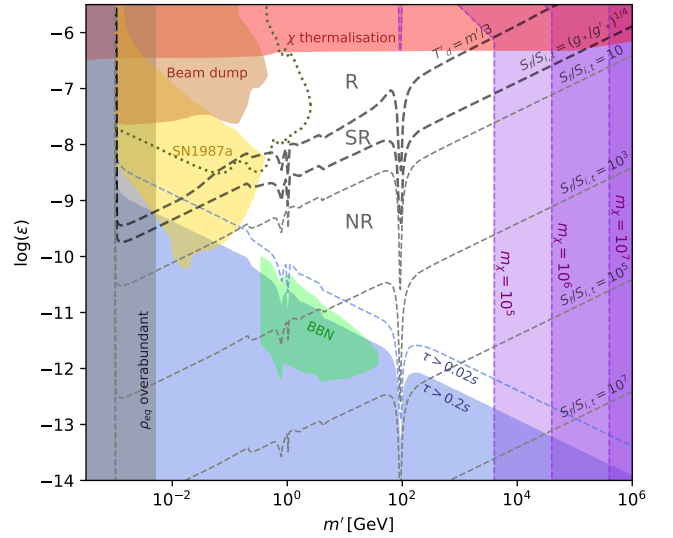


Figure 5: Dark photon parameter space in the scenario with an initially dominant dark sector ($\xi_i \gg 1$). Constraints include present (brown) and expected future (green dotted) beam dump experiments [48], supernovae (yellow) [49] and the BBN bound computed in [44] (bright green). Candidates in the blue region are overabundant at $T = 1$ MeV ($\rho'/\rho_t > 0.04$). DM has thermalized with the VS for the candidates in the red region. In the purple region (whose boundary depends on the DM mass, m_{dm}), the dark photons have thermalized before the DM freeze-out.

next section.

A. Reheating after DM freeze-out

The cosmological scenario we consider essentially rests on two hypotheses. First, we assumed that the Universe was dominated by a hot HS, $\xi \gg 1$, before BBN. Second, we assumed that during that period, the DM abundance was set by secluded thermal freeze-out, through $\chi\bar{\chi} \rightarrow \gamma'\gamma'$ processes. Concretely, we require that the hidden and visible sectors were effectively decoupled so that $\xi \approx \text{constant}$ around DM freeze-out. The processes that could lead to the thermalization of the two sectors are γ' decay and inverse decay on one hand, and DM annihilation (production) into (from) VS particles on the other hand. We begin with the latter.

Considering annihilation, we consider $\chi\bar{\chi} \leftrightarrow f\bar{f}$ [11] and require that these processes were out of equilibrium at $T' \approx m_{\text{dm}}$, here the mass of the χ particle. That moment gives the strongest constraint because the annihilation rate $\Gamma_{f\bar{f}}/H \propto 1/T' \sim a$ when the DM particles were relativistic, but Boltzmann suppressed when they became non-relativistic, so the maximum lies around $T' \approx m_{\text{dm}}$ [31, 50]. The condition that the two sectors

do not equilibrate at that moment is $\Gamma_{f\bar{f}} \lesssim H(m_{\text{dm}})$ or

$$\varepsilon \lesssim \left(\frac{m_{\text{dm}}}{\alpha' m_{\text{Pl}}} \right)^{1/2} \quad (\text{no } \chi \text{ thermalization}) \quad (36)$$

As we assumed that DM abundance is set by secluded freeze-out of χ into dark photons, $\alpha'^2/m_{\text{dm}}^2 \sim \langle \sigma v \rangle \sim \text{pbarn}$ can be traded for the DM abundance (see below for the possible effects of entropy dilution). This leads to an upper bound on the mixing parameter of $\varepsilon \lesssim 10^{-6}$, corresponding to the red region in fig. 5. The simple estimate neglects the fact that γ' decays produce entropy and thus dilutes the DM abundance, but this effect (including in the relativistic regime) is taken into account in fig. 5. As smaller values of α'/m_{dm} are required (weaker annihilation cross section), the bound on ε is weaker. For $\varepsilon \sim 10^{-6}$, the effect becomes relevant for $m' \gtrsim 10^5$ GeV and leads to a slight rise in the bound on ε .

Next we require that the dark photons have not thermalized with the VS at the time of DM freeze-out, $x'_{\text{fo}} = m'/T'_{\text{fo}}$, so that freeze-out is indeed secluded. The relevant process is $\gamma' \leftrightarrow f\bar{f}$, with rate Γ' in the dark photon rest frame. If we assume that the dark photons are relativistic at DM freeze-out, we require that the thermalization temperature given in eq.(18) is such that $T'_{\text{rh}} \lesssim T'_{\text{fo}} = m_{\text{dm}}/x'_{\text{fo}}$. For $\Gamma' \sim \varepsilon^2 m'$, this gives

$$\varepsilon m' \lesssim 30 \left(\frac{m_{\text{dm}}^3}{m_{\text{Pl}} x'_{\text{fo}}} \right)^{1/2} \quad (\text{no } \gamma' \text{ thermalization}) \quad (37)$$

which depends both on m' and m_{dm} . As in (36), the dependence on the DM mass can be traded for the DM abundance, but that would leave a dependence on the HS fine structure constant. Furthermore, we impose that $m' \lesssim m_{\text{dm}}/x'_{\text{fo}}$, so that the dark photons are still essentially relativistic at the moment DM freeze-out. The bound from non-thermalization of dark photons is in purple in fig.5, combining constraint (37) with $m' \lesssim m_{\text{dm}}/x'_{\text{fo}} \approx m_{\text{dm}}/20$.

B. Experimental and astrophysical constraints

For fixed m' , a lower bound on ε comes from BBN constraints. The dark photons must be non-relativistic before BBN to avoid contributing too much to the expansion rate. This is often expressed in terms of the effective number of neutrino-like degrees of freedom, ΔN_{eff} . Here, we find it more directly relevant to impose that $\rho'/\rho_{\text{sm}} < 0.04$ at 95% confidence at BBN [51, 52].

We noted in section III A 3 that thermalization before BBN is a necessary but not sufficient condition if it occurs while the dark photons are still relativistic. After thermalization, the dark photons remain in thermal equilibrium with the VS. If they are still relativistic during BBN, then $\rho'/\rho_{\text{SM}} = g'_*/g_* \approx 0.3$, which is excluded. Thus, they must be non-relativistic. Requiring $\rho'/\rho_{\text{sm}} <$

0.04 sets the lower bound $m' \approx 5$ MeV, corresponding to the shaded vertical line in fig. 5. If, instead, the dark photons become non-relativistic during the heating of the VS, then the constraint from BBN is essentially that dark photons decay before BBN. Here, $\rho'/\rho_{\text{sm}} < 0.04$ so long as $\tau' < 0.2$ sec, so the blue region is excluded in fig. 5, with a boundary such that $\varepsilon \propto m'^{-1/2}$. The dip around ~ 90 GeV is due to the degeneracy between the γ' and the Z boson. Extra features correspond to hadronic bound states. To compute the decay rate of the γ' into hadrons, we have followed section IV of [44] using the R-ratio, $\Gamma(\gamma' \rightarrow \text{hadrons}) = R(E_{\text{cm}} = m')\Gamma(\gamma' \rightarrow \mu\bar{\mu})$. For reference, we also show the bound from a shorter lifetime, $\tau' = 0.02$ s, with the dashed blue line. For this lifetime, thermalization of the dark photons at BBN is only a secondary issue as the expansion is essentially dominated by the SM. It may happen that the dark photons end up thermalizing with the SM if inverse decay processes are significant, see section III B and appendix E. Regardless, after decay, $\rho' \ll \rho$ and the dark photons are totally subdominant.

Finally, we show the terrestrial collider, beam dump experiments and astrophysical observations that set relevant bounds on γ' mixing and mass. The most sensitive current limits come from E137 [53], LSND [54], CHARM [55] and NuCal [56, 57], see [48] for a summary. These are shown in brown and yellow in fig.5, while the expected improved bounds from SHiP [58] are given by the green dotted line. In turn, the most relevant astrophysical bound comes from the measurement of the timescale of the neutrino burst from SN1987A. The limit we show in yellow in fig.5 is taken from an analysis by Ref. [49]. The light green region is from the analysis of [44], which considered that the γ' is produced through freeze-in so their abundance satisfies the bound $\rho'/\rho_{\text{sm}} < 0.04$. Their analysis used a more sophisticated criteria to constraint γ' decay around BBN.

Combining all the constraints discussed in this section, the available mass and mixing parameter space for a γ' assuming an initially hot HS, i.e. $T' \gg T$, corresponds to the white region of fig.5.

C. Entropy production

The entropy produced from a hot HS can be very substantial. In fig.5, the upper thick black dashed line (R-NR boundary) corresponds to a thermalization temperature such that $3T'_{\text{th}} = m'$, see eq.(19). This is a convenient criteria to delineate relativistic and non-relativistic temperatures (again assuming MB statistics). From $3T'_{\text{th}} = m'$ and eq.(19), we see that the boundary scales as $\varepsilon \propto m'^{1/2}$, except for γ' masses for which it mixes with the Z or hadronic resonances in the photon channel. This line crosses the constraint from DM thermalization, $\varepsilon \lesssim 10^{-6}$, around $m' = 1$ TeV, and the one from BBN around $m' = 5$ MeV and $\varepsilon \sim 10^{-9}$. To the left of that line, thermalization occurs when the dark

photons are relativistic (R). For fixed m' , the larger the ε , the larger the reheating temperature, $T_{\text{rh}} \propto \varepsilon$. Conversely, for fixed ε , the larger the dark photon mass, the larger $T_{\text{rh}} \propto m'^{2/3}$ (see eq.(18)). The maximal T_{rh} is reached around 1 TeV. The lower end corresponds to a HS and VS that thermalize just before BBN, with $m' \sim$ few MeV.

The separation between the relativistic and non-relativistic scenarios of γ' decay is not clear cut. Another possible criteria to separate the two regimes is entropy production. $S_{t,f}/S_{t,i} \approx (g_*/g'_*)^{1/4}$ in the case of relativistic thermalization, while $S_{t,f}/S_{t,i} \approx (g_*/g'_*)^{1/4}(\tau'/t_{\text{nr}})$ in the non-relativistic regime, where $t_{\text{nr}} \sim m_{\text{pl}}/m'^2$ is the time when the dark photons become non-relativistic, see sections III A 4 and III B 2 and appendix B. In fig.5, the lower thick black dashed line is set by requiring that $S_{t,f}/S_{t,i}$ departs from $(g_*/g'_*)^{1/4}$. The region below it corresponds thus to non-relativistic decays, with significant entropy production. The fact that the lower dashed curve does not scale like the upper dashed one is due to changes in g_* . We call the region between the two thick dashed lines semi-relativistic (SR), a part of the parameter space that could not be covered by our approximate analytical solutions. Contours of constant $S_{t,f}/S_{t,i}$ are shown as thinner dashed lines. Thus, for a large part of the allowed dark photon domain, the entropy dilution factor can be important. This has an impact not only on the DM abundance, but also on any relics which may lie within the VS, such as a baryon asymmetry (see section V C).

V. DOMAIN OF THERMAL DM CANDIDATES

We now examine the impact of heating of the VS on the domain of thermal DM candidates [31]. To recap, the domain delineates in the plane $\xi_{\text{fo}} - m_{\text{dm}}$ all possible DM candidates that were in thermal equilibrium in a HS. Its construction is based on generic assumptions, such as the unitarity bound on the DM annihilation cross section. Among other things, it was assumed in [31] that the universe was RD from DM freeze-out to BBN. In the language of the present work, this means that the DM companion particles were still relativistic at reheating, see sections III A-IV and fig.5. In that case, entropy dilution is $S_{t,f}/S_{t,i} \approx (g_*/g'_*)^{1/4} = \mathcal{O}(1)$ [31]. One of our motivations was to check to what extent this is possible. As fig.5 shows, a large part of the γ' parameter space corresponds to relativistic reheating.

Heavier and more feebly coupled dark photons leads to non-relativistic reheating, see section III B. In that case, entropy production can be very important, causing dilution both of possible relics from the VS and of DM itself. Provided this can be made consistent with a baryogenesis mechanism, such entropy production greatly expands the boundaries of the domain to larger DM masses, both for the case of a hot HS, $\xi \gtrsim 1$, and for a cold HS, $\xi \lesssim 1$.

A second generalisation of the results of [31] regards the treatment of the temperature ratio at DM freeze-out, ξ_{fo} . In [31], this was treated as a free parameter and it was assumed that $\xi \approx \xi_i$ is well defined or, in terms of the present work, that the HS and VS were effectively decoupled around DM freeze-out. As we have seen in III A 1, this occurs so long as the initial heating parameter satisfies $\kappa_i \sim (\rho'_i/\rho_i)\langle\Gamma'_i\rangle/H_i \lesssim 1$. If this is not the case, the HS heats up the VS to a maximal temperature, T_{max} , while ξ falls very rapidly. As we shall see, imposing that the HS and VS were decoupled at DM FO sets a new bound on both the maximal and minimal values of ξ_{fo} as a function of the DM mass. That maximal bound is stronger than the one set in [31] using the constraint from ΔN_{eff} at BBN. These results, which are detailed in this section, are summarised in fig.6, extending the analysis of [31]. It also includes features that are relevant if baryogenesis takes place before reheating and depicts various dark QED DM candidates, for fixed values of α' .

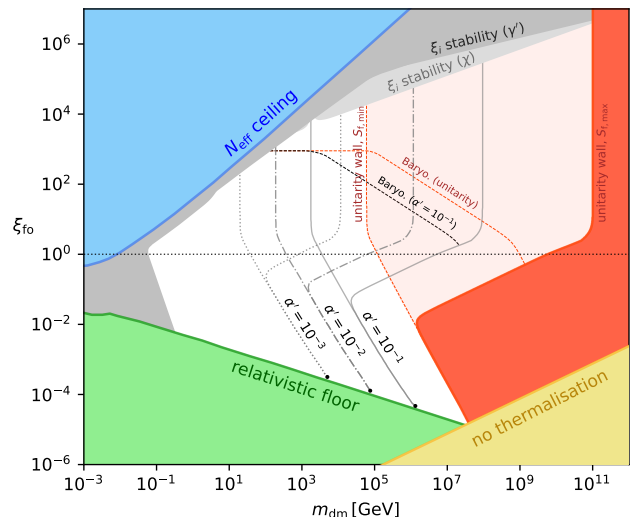


Figure 6: The domain of thermal dark matter candidates, taking into account reheating of the VS. The relativistic floor, N_{eff} ceiling and no thermalization bounds have already been discussed in [31], and are not impacted. The unitarity wall (red), which accounts for maximum possible dilution, is shifted to the right with respect to the case of minimum dilution (dashed red line). The same limits in non-unitary cases (i.e. dark QED), for $\alpha' = 10^{-1}$, 10^{-2} and 10^{-3} are shown by the three grey lines (dotted, dot-dashed and solid). As for the unitarity wall, the different curves branch off when entropy production can become significant. The grey ξ_i stability conditions ensure that the initial conditions are stable at the beginning of the scenario. The constraint from baryogenesis, discussed in section V C, is displayed in dashed red (for the case of unitary cross section) and black (for $\alpha' = 0.1$).

A. Unitarity wall

A DM particle that is non-relativistic at freeze-out has a relic abundance that scales as $\Omega_{\text{dm}} \propto 1/\langle\sigma v\rangle$. Assuming a 2-to-2 process, its annihilation cross-section is bounded from above by unitarity [32]

$$\sigma v \leq \frac{4\pi(2J+1)}{m_{\text{dm}}^2 v}. \quad (38)$$

Therefore $\Omega \propto m_{\text{dm}}^2$, and this sets an upper bound on the DM mass, $m_{\text{dm}} \lesssim 150$ TeV for s-wave ($J=0$) and assuming SM degrees of freedom only. This is the unitarity bound, it provides a simple and useful way to delineate the possible thermal DM candidates. It is important to keep in mind that higher DM masses are possible, for instance when several partial waves beyond s-wave are relevant, a generic feature for multi-TeV DM candidates [59, 60]. Here, as in [31], we impose the bound (38) assuming s-wave for simplicity and focus on the impacts of ξ and of possible entropy dilution.

That the unitarity bound may depend on ξ_i is fairly intuitive. If $\xi_i < 1$, the DM particles are relatively less abundant than for $\xi_i = 1$ and so can be more massive [31, 61]. Explicitly, this bound on $\xi_i = \xi_{\text{fo}}$ scales like $1/m_{\text{dm}}^2$ in the $\xi_{\text{fo}} - m_{\text{dm}}$ plane, see dotted red curve in fig.6. For fixed ξ_i , a DM particle that is heavier than the unitarity bound is overabundant and thus in principle excluded (the ‘unitarity wall’). The unitarity bound extends to the region $\xi_i \gtrsim 1$. When there is negligible entropy production, the VS plays little role and so the bound is independent of ξ_i . Soon we will turn to the impact of entropy dilution.

Using the instantaneous freeze-out approximation, $n_{\chi,\text{fo}}\langle\sigma v\rangle \approx H_{\text{fo}}$, and taking the s-wave unitarity limit for the annihilation cross section, the DM relic density can be expressed as

$$\Omega_{\text{dm}} h^2 \approx 0.12 x_{\text{fo}}^{1/2} \frac{(g_*/\xi_i^4 + g_*')^{1/2}}{g_{*,s}/\xi_i^3 + g_{*,s}'} \frac{S_{t,i}}{S_{t,f}} \left(\frac{m_{\text{dm}}}{100 \text{ TeV}} \right)^2 \quad (39)$$

for all $\xi_i \approx \xi_{\text{fo}}$. The factor that involves the degeneracy parameters, g_* and g_*' , comes from the expansion rate and entropy density, both taken at freeze-out $\xi_{\text{fo}} \equiv \xi_i$. We also used $\langle 1/v \rangle = x_{\text{fo}}^{1/2}/\sqrt{\pi}$ from MB statistics [31, 32]. Finally, $S_{t,i}$ ($S_{t,f}$) refers to the total co-moving entropy at the initial time (resp. after companion decay), meaning around DM freeze-out. The relation shows that Ω_{dm} is independent of ξ_i for $\xi_i \gg 1$, while $\Omega_{\text{dm}} h^2 \sim \xi_i m_{\text{dm}}^2$ for $\xi_i \ll 1$.

1. Unitarity wall, no entropy dilution

If there is no entropy production, setting $g_* = 10^2$, $g_*' = 3$ and $x_{\text{fo}}' = 20$, the unitarity limit is

$$m_{\text{dm}} \approx 60 \text{ TeV} \quad (40)$$

for $\xi_i \gtrsim 1$ and increases toward larger DM masses for $\xi_i \lesssim 1$,

$$\xi_i \approx \left(\frac{100 \text{ TeV}}{m_{\text{dm}}} \right)^2 \quad (41)$$

see fig.6 and [31]. For fixed ξ_i , $x_{\text{fo}}' = m_{\text{dm}}/T_{\text{fo}}'$ is $\mathcal{O}(20)$, characteristic of non-relativistic DM freeze-out. However, it can be shown that the DM are less non-relativistic at freeze-out as ξ_i decreases [31].

Another significant bound in the domain is the *relativistic floor* [61], the green region of fig.6. This corresponds to DM particles that freeze-out when they were relativistic, like the SM neutrinos. In that case, $\Omega_{\text{dm}} \sim \xi_i^3 m_{\text{dm}}$ and so $\xi_i \propto 1/m_{\text{dm}}^{1/3}$. Candidates below the relativistic floor are in principle under-abundant and thus are excluded, hence the name of the bound. Where the unitarity wall and the relativistic floor meet the hypothesis that the DM particles were initially in thermal equilibrium breaks down and so that region (in yellow) is also excluded [31, 61].

We now consider the impact of possible entropy dilution. While this depends on the properties of the DM companion, it is possible to draw some generic conclusions, building on what we have learned for the case of a dark photon.

2. Unitarity wall with entropy dilution, $\xi_i \gtrsim 1$

Let us begin with $\xi_i \gtrsim 1$ and consider a companion particle that is still relativistic at VS reheating. In this case, the entropy produced only depends on the ratio of the numbers of degrees of freedom of the VS and the DM companion particle, $S_{t,f}/S_{t,i} \approx (g_*/g_*')^{1/4}$. For a massive dark photon, $g_*' = 3$, so for $g_* \approx 10^2$ we have $S_{t,f}/S_{t,i} \approx 2.4$. Here, the HS and VS thermalize and the DM companion remains with the SM in thermal equilibrium after reheating. The constraints from BBN requires that the companions are heavier than a few MeV [52]. If they meet these conditions, the DM candidate is viable. The unitarity bound on the DM mass is shifted toward a larger maximal DM mass by a factor of $(g_*/g_*')^{1/8} \sim \mathcal{O}(1)$ [31, 42].

Consider now $\xi_i \gtrsim 1$, but with a DM companion that is non-relativistic at VS reheating. In that case, significant entropy can be produced. If there is one DM companion, the entropy produced through its decay depends on its lifetime, τ' , and the time t_{nr} when it becomes non-

relativistic, see eq.(B11):

$$\frac{S_{t,f}}{S_{t,i}} \simeq \left(\frac{g_*}{g'_*}\right)^{1/4} \left(\frac{\tau'}{t_{\text{nr}}}\right)^{1/2} \quad (\xi_i \gtrsim 1) \quad (42)$$

This reduces to $S_{t,f}/S_{t,i} \simeq (g_*/g'_*)^{1/4}$ if, as in the previous paragraph, reheating occurs when the companion is still relativistic, $t_{\text{nr}} \gtrsim \tau'$. Setting $g'_* = 3$ and $g_* = 10^2$ for simplicity, this is rewritten as

$$\frac{S_{t,f}}{S_{t,i}} \approx 4 \left(\frac{m'}{10 \text{ MeV}}\right) \left(\frac{\tau'}{0.2 \text{ s}}\right)^{1/2} \quad (\xi_i \gtrsim 1) \quad (43)$$

with $\tau' \lesssim 0.2$ s, a benchmark value that corresponds roughly to BBN time [51]. The dependence on m' arises from $t_{\text{nr}} \sim 1/H \propto 1/m'^2$ for $\xi_{\text{nr}} \gg 1$. Assuming the unitarity limit, the relic abundance reads

$$\Omega_{\text{dm}} h^2 \approx 0.12 \left(\frac{m_{\text{dm}}}{100 \text{ TeV}}\right)^2 \left(\frac{10 \text{ MeV}}{m'}\right) \left(\frac{0.2 \text{ s}}{\tau'}\right)^{1/2}. \quad (44)$$

Maximum entropy is produced when the companion is as heavy as possible and has the longest lifetime compatible with BBN. For the companion mass, we take $m' \sim T'_{\text{fo}} \sim m_{\text{dm}}/20$, so that it becomes non-relativistic right at DM freeze-out. The unitarity bound is then

$$m_{\text{dm}} \lesssim 10^{11} \left(\frac{\tau'}{0.2 \text{ s}}\right)^{\frac{1}{2}} \text{ GeV} \quad (\xi_i \gtrsim 1, \text{ unitarity}) \quad (45)$$

Taking $\tau' \approx 0.2$ s gives the vertical part of the red region in fig. 6 (maximal entropy production). Comparing with a scenario in which the companion is relativistic at reheating (minimal entropy production), we conclude that the light red region encompasses all DM candidates with unitarity limit annihilation cross section and a lifetime that varies from $\tau' \sim 0.2$ s (maximal entropy dilution) to $\tau' \lesssim t_{\text{nr}}$ (minimal entropy dilution). Note that the DM can be much more massive than is usually assumed based on unitarity [33, 42]

This concerns DM with unitarity limit annihilation cross section (which we called unitary candidates). In the same figure 6, we give contours of constant $\Omega_{\text{dm}} h^2 \approx 0.12$ for dark QED DM candidates for various values of the dark fine structure constant α' . As for the unitary candidates, the vertical parts of the curves correspond to minimal, $S_{t,\text{min}}$, and maximal, $S_{t,\text{max}}$, entropy production. The latter corresponds to dark photons that become non-relativistic around DM freeze-out, $m' \sim m_{\text{dm}}/x'_{\text{fo}}$ and have maximal lifetime, $\tau' \sim 0.2$ s. The former corresponds to dark photons that thermalize with the VS when they are still relativistic. Between each of these lines, there is a continuum of DM candidates, corresponding to different choices of dark photon mass and decay lifetime (or kinetic mixing parameter).

3. Unitarity wall with entropy dilution, $\xi_i \lesssim 1$

Consider next $\xi_i \lesssim 1$, meaning a cold HS. Although the main part of our work is focused on a hot HS ($\xi_i \gg 1$), we want to understand how this region interpolates with the unitarity wall of eq.(45). If $\xi_i \ll 1$, we would expect that the companion plays a minimal role, unless it is stable or very long-lived or, alternatively, it is unstable but comes to dominate the expansion of the universe before its decay, thus producing entropy. We start with the former and consider a light but stable DM companion. Putting aside the possibility that the companion has interactions and could undergo a phase of cannibalism [62], its relic abundance is akin to that of DM particles that decouple when they are still relativistic [31, 61]

$$\Omega' h^2 \approx 0.12 g' \frac{g_{*s,0}}{g_{*s,\text{fo}}} \xi_i^3 \left(\frac{m'}{6 \text{ eV}}\right) \quad (46)$$

The factor $g_{*s,0}/g_{*s,\text{fo}}$ takes into account entropy dilution from within the VS, but essentially $\Omega' \sim m' \xi_i^3$. As the relativistic floor corresponds to DM candidates with $\Omega_{\text{dm}} h^2 \approx 0.12$, fixing ξ_i , we conclude that a stable or very long lived dark photon is viable if its mass lies to the left of the relativistic floor, in such a way that $\Omega' h^2 \lesssim 0.12$.

Consider finally $\xi_i \ll 1$ with an unstable DM companion that becomes non-relativistic (t_{nr}) and comes to dominate the expansion (t_{eq}). In that case, as explained in appendix B, the entropy produced is given by

$$\frac{S_{t,f}}{S_{t,i}} \approx \frac{\rho'_{\text{nr}}}{\rho_{\text{nr}}} \left(\frac{\tau'}{t_{\text{nr}}}\right)^{1/2} \quad (47)$$

see eq.(B12). Note that this expression, which is valid provided $S_{t,f}/S_{t,i} \gtrsim 1$, differs from eq.(42) by a factor $\sim \xi_{\text{nr}}^4$ which is much smaller than 1 for $\xi_i \ll 1$. Yet, entropy production can be large if the companion is long-lived. As above, using the benchmark values $g' = 3$ and $g = 10^2$, we express this as

$$\frac{S_{t,f}}{S_{t,i}} \approx 0.1 \xi_i^3 \left(\frac{m'}{10 \text{ MeV}}\right) \left(\frac{\tau'}{0.2 \text{ s}}\right)^{1/2} \quad (48)$$

This is to be compared with eq.(43), from which we see that entropy production requires heavier companion mass if $\xi_i \ll 1$.² Consequently, for $\xi_i \ll 1$, assuming

² This assumes that the abundance of dark companions is fully characterised by ξ_i . In other words, we assume that their abundance is not affected by production of companions from VS particles through freeze-in processes. The case of dark photons is instructive, see appendix E. As is well-known, abundances through freeze-in processes are controlled by $Y' \sim \Gamma'/H(m') \ll 1$. At the same time, entropy production is maximized when the companions are long-lived, and scales as $(\tau'/t_{\text{nr}})^{1/2} \sim (H(m')/\Gamma')^{1/2}$. These two effects being antagonist, the entropy produced from

unitarity annihilation cross section and entropy dilution, the DM abundance reads

$$\Omega_{\text{dm}} h^2 \approx \frac{0.12}{\xi_i^2} \left(\frac{m_{\text{dm}}}{100 \text{ TeV}} \right)^2 \left(\frac{10 \text{ MeV}}{m'} \right) \left(\frac{0.2 \text{ s}}{\tau'} \right)^{1/2} \quad (49)$$

This expression, which applies for $\xi_i \ll 1$, is to be compared with eq.(44), which is valid for $\xi_i \gg 1$. It contains an extra factor of $1/\xi_i^2$, which stems from eq.(39) taking into account entropy production. Both expressions match for $\xi_i \sim 1$. As for the case $\xi_i \gg 1$, we see that entropy dilution is maximal if both the companion mass and its lifetime are as large as possible. Taking, as before, $m' \sim m_{\text{dm}}/x'_{\text{fo}}$ and $\tau' \approx 0.2 \text{ s}$ (maximal entropy production) gives the part of the unitarity wall that scales as

$$\xi_i \approx \left(\frac{m_{\text{dm}}}{10 \text{ EeV}} \right)^{1/2} \quad (\text{max. entropy dilution}) \quad (50)$$

see fig.6. The maximum allowed DM mass m_{dm} for $\xi_i = 1$ is about $6 \times 10^9 \text{ GeV}$, similar to values quoted in [33]. We found that entropy dilution may become relevant for $\xi_i \approx 10^{-2}$ and $m_{\text{dm}} \approx 10^6 \text{ GeV}$, where the red curves separate in two branches, one corresponding to minimal and the other one to maximal entropy dilution. For smaller values of ξ_i , entropy dilution is always negligible in the sense that the companion abundance is so low that it never comes to dominate the expansion of the universe and so cannot produce significant entropy. In that case the unitarity wall is as given by eq.(41).

Again, we have focused on the impact of entropy dilution on the unitarity wall, but clearly the same features arise for specific DM candidates. Fig.6 shows contours of constant $\Omega_{\text{dm}} h^2 \approx 0.12$ curves for different cases of dark QED. We see the similar branching between DM candidates with little entropy production ($S_{\text{t,min}}$), and those with maximal entropy production, ($S_{\text{t,max}}$), with a continuum of candidates between the two branches. We also observe that when the fine structure constant decreases and the curves move toward the left part of the domain, the gap between the branches shrinks. This is because the maximal amount of entropy that can be produced decreases as the dark photon mass decreases.

B. Stability of ξ_i

One of the basic assumptions underlying the domain depicted in fig.6 is that the initial temperature ratio between the HS and VS is a well-defined parameter. Concretely, we will require that at early times (i.e. around the

time of DM freeze-out) the temperature ratio does not evolve rapidly, $\xi \approx \xi_i$. We have called this the plateau in previous sections. In section III A 2, we introduced the ‘heating parameter’ κ , see eq.(13). We showed that this simple parameter controls the onset of heat transfer from the HS to the VS. If initially $\kappa_i \lesssim 1$, then there is a plateau, $\xi \approx \xi_i$. If instead $\kappa_i \gtrsim 1$, the energy transfer from the HS to the VS is efficient and the temperature of the VS (ξ) rapidly increases (resp. decreases) to some maximal temperature, superseding the initial VS temperature T_i , see purple curve in fig.2. This is for $\xi_i \gg 1$ but a similar condition holds for $\xi_i \ll 1$, the difference being that the role of the VS and HS are reversed. We begin by considering the case $\xi_i \gg 1$.

We now use the heating parameter to impose an extra condition on the domain by requiring that the initial temperature ratio is stable. For $\xi_i \gg 1$, we demand

$$\kappa_i \approx \frac{\rho'_i \langle \Gamma' \rangle_i}{3\rho_i H_i} \lesssim 1 \quad (51)$$

at $T'_i \approx m_{\text{dm}}/x'_{\text{fo}}$. This corresponds to

$$0.05 \xi_i^4 \left(\frac{m'}{10 \text{ MeV}} \right) \left(\frac{\text{GeV}}{m_{\text{dm}}} \right)^3 \left(\frac{0.2 \text{ s}}{\tau'} \right) \lesssim 1. \quad (52)$$

Again, we set $g_* = 10^2$, $g'_* = 3$ and $x'_{\text{fo}} \equiv x'_i = 20$ to avoid cluttering; the factor m'/m_{dm} is due to time dilation. This condition depends on m' and τ' . These parameters can be eliminated by noting that the condition is the weakest, thus leaving the largest domain, provided m' is as light as possible and τ' as long as possible. As we have seen, we must require that the companion decays and is non-relativistic before BBN. Taking $m' \approx 5 \text{ MeV}$ and $\tau' = 0.2 \text{ s}$ and assuming no entropy production gives

$$\xi_i \lesssim \left(\frac{m_{\text{dm}}}{100 \text{ MeV}} \right)^{3/4} \quad (\xi_i \gtrsim 1, \text{ no entropy dilution}) \quad (53)$$

This condition corresponds to the grey region depicted in fig.6 for $m_{\text{dm}} \lesssim 100 \text{ TeV}$ and $\xi_i > 1$.

Heavier DM candidates are possible, provided there is entropy dilution. Within the the red-shaded region, we impose stability of ξ_i making also sure that the companion decay will produce the right amount of entropy. Here the dark sector is largely dominant, so the expression (44) holds, in which we can isolate m' and inject it into (52) to obtain

$$\xi_i \lesssim 10^5 \left(\frac{m_{\text{dm}}}{100 \text{ TeV}} \right)^{1/4} \quad (\xi_i \gtrsim 1, \text{ with entropy dilution}) \quad (54)$$

The two conditions cross each other at $m_{\text{dm}} \sim 100 \text{ TeV}$, as expected.

The same consideration applies to the DM particle themselves. Concretely, we must also make sure that substantial energy transfer does not happen before DM freeze-out via DM-SM particles scatterings. To do so,

particles that are produced through freeze-in is at most $\mathcal{O}(1)$. In other words, we can safely assume that, when entropy production may be substantial, the abundance of dark companions is fully determined by the initial condition ξ_i . We have also checked this numerically.

similarly to the condition on the heating parameter for dark photon decay, we require that

$$\kappa_{\text{dm}} \sim \frac{\rho_{\text{dm}}}{\rho} \frac{\Gamma}{H} \Big|_{T' \sim m_{\text{dm}}} \lesssim 1 \quad (55)$$

with $\rho_{\text{dm}}/\rho \sim \xi^4$ and here $\Gamma \sim \alpha\alpha'\varepsilon^2 m_{\text{dm}}$ is the interaction rate between DM and SM particles around $T' \sim m_{\text{dm}}$. To make this condition as conservative as possible we set $m' = m_{\text{dm}}/x'_{\text{fo}}$ and $\tau' = 0.2\text{s}$, and determine the value of α' by requiring the right relic abundance for a non-relativistic freeze-out [13]:

$$\Omega_{\text{dm}} h^2 \simeq 10^9 \frac{x_{\text{fo}}}{g_*'^{1/2} m_{\text{Pl}} \langle \sigma v \rangle} \frac{S_{t,i}}{S_{t,f}} = 0.12 \quad (56)$$

with $\langle \sigma v \rangle \sim \alpha'^2/m_{\text{dm}}^2$ the annihilation of DM into dark photons. In that case, where the DS is dominant, the entropy production due to dark photons decay follows (B11). Taking the same values for g_* , g_*' and $x'_{\text{fo}} \sim 20$ as usual, we obtain the condition³

$$\xi_i \lesssim \left(\frac{m_{\text{dm}}}{100\text{eV}} \right)^{3/8} \quad (\xi_i \gtrsim 1, \text{ with entropy dilution}) \quad (57)$$

which is depicted by the light grey region in figure 6, labeled ξ_i stability (χ).

Next, we consider a cold HS, $\xi_i \lesssim 1$. In that scenario, it is possible that the HS is completely secluded (i.e. $\varepsilon \rightarrow 0$) provided the dark photon mass lies within the relativistic floor (see above). If not, the dark photon should decay into SM particles and this without spoiling the abundance of elements produced by BBN. This problem is beyond our scope (but is work in progress). Here we focus on the stability of the initial temperature ratio. The reasoning of section III A 2 straightforwardly applies, provided the role of the two sectors are inverted, that is $\rho' \leftrightarrow \rho$. This leads to the following condition for the stability of ξ_i

$$\kappa'_i \approx \frac{\rho_i}{3\rho'_i} \frac{\langle \Gamma' \rangle}{H_i} \lesssim 1. \quad (58)$$

In this expression, the relevant rate is driven by the conditions of the VS. Assuming, as for the dark photon, that the relevant process for energy transfer from the VS to the HS is production through inverse decay, we have $\langle \Gamma' \rangle \sim m' \Gamma' / T$. In plain words, the condition of stability is simply that freeze-in production can be neglected at the time of DM freeze-out, $\xi_{\text{fo}} \equiv \xi_i \ll 1$. With the same approximations as before on g_* , g_*' and x'_{fo} , and the same

choice for m' and τ' , this gives

$$\xi_i \gtrsim \left(\frac{100 \text{ MeV}}{m_{\text{dm}}} \right)^3 \quad (\xi_i \lesssim 1) \quad (59)$$

see grey region for $\xi_i \ll 1$ in fig.6. For $\xi_i \ll 1$, entropy production is only relevant for much heavier dark companions. As explained above, for such particles, production through freeze-in is negligible, see appendix E.⁴ Finally, we have checked that the freeze-in production of DM lead to a condition of stability that is parametrically weaker than that from the freeze-in of dark photons.

C. Comments on baryogenesis

From BBN and CMB anisotropies, the baryon-to-photon ratio of the Universe is [63], $\eta \equiv n_b/n_\gamma \approx 6 \cdot 10^{-10}$, corresponding to a baryon number $B = (n_b - n_{\bar{b}})/s \approx 10^{-10}$ in the early Universe, a tiny number that could be explained through some baryogenesis mechanism [13]. In most scenarios, baryogenesis is supposed to take place in the very early Universe, through the decay of some very heavy particle, like in leptogenesis [64], at the electroweak scale [65] or from some baryon-number charged scalar field (Affleck-Dine) [66]. However, motivated by a low reheating scenario [25], there are also baryogenesis mechanisms that try to explain the generation of the baryon asymmetry at temperatures as low as \sim few MeV, see e.g. [67] and references therein. Assuming the former class of mechanisms, a hot HS has several interesting implications for baryogenesis.

We can parameterize the baryon number at the moment of baryogenesis as $B = \epsilon_B T_B^3 / s_B$ where ϵ_B captures baryon number violation and C and CP violation factors, T_B is the characteristic temperature and s_B the entropy density. On general grounds, ϵ_B is a small number. For instance, if $s_B \sim g_* T_B^3$ with $g_* \sim 10^2$, then $\epsilon_B \sim 10^{-8}$ or so is required to explain the baryon number. Thus ϵ_B is essentially the measure of the produced baryon asymmetry [13]. Baryogenesis scenarios that involve the baryon/lepton number decay of some heavy particle lead naturally to such a small ϵ_B , but in scenarios *à la* Affleck-Dine, the asymmetry can be much larger, possibly $\epsilon_B \sim 1$. Now, if the expansion is driven by a hot HS, $s_B \sim g_*' T_B^3$, so $B \sim \epsilon_B / (g_*' \xi_B^3)$. If thermalization of the VS and HS occurs when the HS particles are

³ This bound is obtained from eq.(55), in which the dependence on the factor ε^2 is eliminated by setting the lifetime of the dark photon to be around BBN (see section IV B and the boundary of the blue region in figure 5)

⁴ Even if the initial temperature $\xi_i \ll 1$ is stable at DM freeze-out, there may be subsequent production of dark companions through freeze-in thus superseding the initial abundance of dark companions, see E. If the dark companion is unstable, as for the case of the dark photon considered in the work, the very same process that lead to dark companions production will lead to their decay. This comes with no or negligible entropy production and so has no impact on the DM abundance and thus on the domain, see footnote 2.

all relativistic, entropy production is mild, $\mathcal{O}(1)$ and the temperature ratio must be such that $\xi_B \approx (10^8 \epsilon_B)^{1/3}$.

We report such constraints in figure 6 by assuming that $\xi_B \sim \xi_i$. Imposing that $\epsilon_B \lesssim 1$ requires that $\xi_i \lesssim 10^3$ (see horizontal part of the dashed lines in fig.6). Once entropy production takes in, the baryon asymmetry is further reduced by a factor $(S_{t,i}/S_{t,f})^{1/3}$. We extract this factor by fixing the DM abundance (see diagonal part of the dashed lines), e.g. using eq.(39) in the unitarity limit. In that case (orange dashed), the bound on ξ_i scales as $\xi_i \lesssim 10^3 (100 \text{ TeV}/m_{\text{dm}})^{2/3}$ for $\xi_i \gg 1$, and $\xi_i \lesssim (1 \text{ EeV}/m_{\text{dm}})^2$ for $\xi_i \lesssim 1$.

A hot HS may also impact the dynamics of baryogenesis. For instance, the condition for out-of-equilibrium decay of some very heavy particle, say N , becomes $\Gamma_N \lesssim H(T \sim m_N) \sim g_*' \xi^2 m_N^2/m_{\text{Pl}}$. Due to the faster expansion rate, the decaying particle could be substantially lighter. With $\Gamma_N \sim \alpha_N m_N$, the condition for out-of-equilibrium decay then becomes $m_N \gtrsim \alpha_N m_{\text{Pl}}/\xi^2$. Note that if the inflaton decay dominantly heats the HS, imposing $T'_{\text{th}} \lesssim 10^{15} \text{ GeV}$ [68] requires only that $T'_{\text{th}} \lesssim 10^{15}/\xi \text{ GeV}$. In a different class of scenarios, baryon-number violating processes around the electroweak phase transition is also affected if the expansion of the Universe is non-standard [69]. As mentioned above, the temperature for relativistic thermalization may lie somewhere between a few MeV and around 1 TeV. That range includes the scale for EW breaking, $T_c \sim 100 \text{ GeV}$ [70], so it may have occurred while the expansion was dominated by a hot HS, impacting scenarios for EW baryogenesis. In particular, the rate for sphaleron transitions in the unbroken phase is $\Gamma_s \sim \alpha_W^5 T$ [71] while $H \sim g_*'^{1/2} T'^2/m_{\text{Pl}}$, so if there is a hot HS, they are efficient at lower temperatures, $T \lesssim 10^{10} \text{ GeV}/\xi^2$. In the broken phase, their rate is Boltzmann suppressed, $\Gamma_s \propto \alpha_W^5 T e^{-E_s/T}$ with $E_s \sim m_W/\alpha_W$. In scenarios with a first order EW phase transition, sphalerons are typically required to be out-of-equilibrium inside bubbles of true vacuum [65]. This condition can be expressed as a condition on the jump of the vev v_b of the Higgs field at the moment of bubble nucleation, $v_b/T_c \gtrsim 1$ [69, 71]. If the expansion is dominated by a hot HS, sphaleron processes are more easily out-of-equilibrium, thus relaxing the bound on the change of the Higgs field. A direct adaptation of the argument in [69], see Eqs.(3,4), gives $v(T_b)/T_c \gtrsim (0.6, 0.8, 0.9)$ for $\xi = (10^3, 10^2, 10)$ respectively.

VI. CONCLUSIONS

We have studied the possibility that, some time before big bang nucleosynthesis, the expansion of the Universe was dominated by a hot hidden sector, with $T' \gg T$. We furthermore assumed that this HS contains a dark matter particle with an abundance that is set by secluded thermal freeze-out through annihilation into a lighter particle, the DM companion. This setup is by and large

motivated by [31], in which the domain of possible thermal DM particle candidates has been delineated in the plane ξ vs m_{dm} . The key issue that we have studied is the fate of the companion, in particular how its energy is transferred to Standard Model particles and the overall impact on the domain of dark matter candidates.

Reheating of a VS is a standard problem in cosmology. Our analysis complements the study of similar scenarios in the literature [15, 33, 42]. First and foremost, we have systematically studied the history of the hot HS, starting from $\xi_i = T'_i/T_i \gg 1$, down to reheating of the VS and the subsequent thermalization of the DM companion. We did so both numerically and analytically, using for the sake of concreteness the framework of dark QED coupled to the SM through kinetic mixing. In brief, we have distinguished two scenarios, which we dubbed relativistic and non-relativistic reheating, depending on whether the companion was relativistic or non-relativistic at the end of reheating. We also emphasized the relevance of a specific combination of rates and energy densities that controls the process of energy transfer and which we called the heating parameter, see eq.(6). Finally, we have articulated these two scenarios to the all important production of entropy [13]. Our main results regarding the process of reheating from a hot HS are illustrated by figure 3 (see also 1).

Next, we have used our results to delineate the parameter space of the dark photons on one hand, cf. figure 5, and the domain of thermal DM candidates on the other hand, see fig. 6. One of our main results is that thermal dark matter candidates from a hot HS could be very heavy, $\lesssim 10^{11} \text{ GeV}$ (see also [15, 33, 42]), much heavier than the standard unitarity upper bound on the WIMP mass [32]. Similar conclusions extend to the case $\xi_i \lesssim 1$. While the HS is subdominant, the DM companion, if sufficiently long-lived, may produce enough entropy to dilute the DM. This can be seen in fig. 6 for $\xi_i \gtrsim 10^{-2}$, see section V for details. Unfortunately, all such DM candidates are very secluded and far beyond the reach of experimental searches. Through their self-interactions mediated by their companion, such secluded DM candidates could be constrained by astrophysical and cosmological observations, see e.g. [50, 62], but as our aim was to be generic, we refrained from reporting specific constraints.

We took the temperature ratio around DM freeze-out, ξ_{fo} , as an initial condition. A natural question is how to embed this within an inflationary scenario. One may argue that it is natural to consider that the inflaton itself is part of a HS. In that respect, it may be natural that reheating after inflation occurs asymmetrically, with initially more heat in the HS than in the VS [15, 21, 72]. An early phase of expansion dominated by a hot HS with $T'/T \approx \text{constant}$ is just one among possible non-standard cosmological scenarios. While we mostly focused on the process of reheating of the VS and on the consequences on the dark photons' parameter space, and more generally on that of thermal DM candidates, it may be of

interest for other cosmological issues. As an example, we briefly discussed the implications for (and constraints from) baryogenesis.

Finally, throughout this work we have made several simplifications to make our equations more tractable and also easier to interpret. First, we used Boltzmann statistics throughout. More importantly, we used a simplified set of Boltzmann equations to describe the energy transfer from the HS to the VS and related the temperatures of both sectors to fluid quantities at equilibrium. While we think that such approximation captures the essence of the process of reheating and the subsequent thermalization of the dark photons, there are features in our numerical solutions that suggest that a more fundamental approach, based on kinetic equations and particle phase space distribution, is called for to properly describe the approach of thermalization. This is work in progress [73].

Acknowledgments

We thank Thomas Hambye and Marco Hufnagel for discussions and collaboration. This work has been supported by the F.R.S./FNRS under the Excellence of Science (EoS) project No. 30820817-be.h “The H boson gateway to physics beyond the Standard Model”, by the FRiA, and by the IISN convention No. 4.4503.15.

Appendix A: Maxwell-Boltzmann statistics

In this work, we made use of simplifications offered by Maxwell-Boltzmann (MB) statistics. First, all basic thermodynamics densities can be expressed in term of simple functions [43]. Also, the chemical potential factors out,

$$n = \frac{g}{2\pi^2} \frac{m^3}{x} K_2(x) e^{\mu/T} \quad (\text{A1})$$

$$\begin{aligned} \rho &= \frac{g}{2\pi^2} m^4 \left[\frac{1}{x} K_3(x) - \frac{1}{x^2} K_2(x) \right] e^{\mu/T} \quad (\text{A2}) \\ &\equiv \frac{g}{2\pi^2} m^4 \left[\frac{1}{x} K_1(x) + \frac{3}{x^2} K_2(x) \right] e^{\mu/T} \end{aligned}$$

$$p \equiv nT = \frac{g}{2\pi^2} \frac{m^4}{x^2} K_2(x) e^{\mu/T} \quad (\text{A3})$$

$$\begin{aligned} s &= \frac{\rho + p - \mu n}{T} \\ &= \frac{g}{2\pi^2} \left(m^3 K_3(x) - \mu m^2 K_2(x) \right) e^{\mu/T}, \quad (\text{A4}) \end{aligned}$$

where the $K_\nu(x)$ are modified Bessel functions and $x = m/T$. Their asymptotic forms are

$$K_\nu(x) \sim \left(\frac{\pi}{2x} \right)^{1/2} e^{-x} \left(1 + \frac{4\nu^2 - 1}{8x} + \mathcal{O}(1/x^2) \right)$$

for large x and

$$K_\nu(x) \sim \frac{1}{2} \Gamma(\nu) \left(\frac{2}{x} \right)^\nu$$

for small x .

The equation of state of a specie is given by

$$w \equiv \frac{p}{\rho} = \frac{K_2(x)}{x K_3(x) - K_2(x)}. \quad (\text{A5})$$

Also, $p = nT$ holds both in the relativistic and the non-relativistic periods using MB. At low temperatures, $m \ll T$, $\rho = mn$ with n the usual density of non-relativistic particles,

$$n = g \left(\frac{mT}{2\pi} \right)^{3/2} e^{-(m-\mu)/T} \quad (\text{A6})$$

while at large temperatures, $T \gg m$,

$$n = \frac{g}{\pi^2} T^3 e^{\mu/T} \quad (\text{A7})$$

$$\rho = 3nT = 3p \quad (\text{A8})$$

$$s = (4 - \mu/T)n \quad (\text{A9})$$

This is where MB departs from Fermi-Dirac (FD) and Bose-Einstein (BE), since the inter-particle separation is of the order of typical wavelengths, $\lambda \sim n^{-1/3} \sim 1/T$, and quantum statistics effect cannot be neglected. However, the error made using MB statistics in this relativistic period is only $\mathcal{O}(10\%)$.⁵

Finally, the mean energy of the particle is given by

$$\langle E \rangle = \frac{\rho}{n} = \frac{\rho_{\text{eq}}}{n_{\text{eq}}} = \begin{cases} m + \frac{3}{2}T & T \ll m \\ 3T & T \gg m \end{cases} \quad (\text{A10})$$

independent of μ . For the thermally averaged decay rate,

⁵ For the sake of comparison, for $\mu = 0$,

$$n_{\text{eq}}/gT^3 = (0.091, 0.10, 0.12)$$

$$\rho_{\text{eq}}/gT^4 = (0.29, 0.30, 0.33)$$

$$s_{\text{eq}}/gT^3 = (0.38, 0.41, 0.44)$$

where the entries refer respectively to FD, MB and BE statistics. MB stands in between FD and BE. This is yet another motivation to use MB: it gives numbers that are midway between fermionic and bosonic particles. While we are comparing different statistics, it is interesting to notice that the relative error made in setting $s = g^{1/4} \rho^{3/4}$ is only (0.04, -0.01, -0.01) again for FD, MB and BE statistics. We make use of this in the appendix on entropy production.

we also need

$$\left\langle \frac{1}{\gamma} \right\rangle = \left\langle \frac{m}{E} \right\rangle = \frac{K_1(x)}{K_2(x)} = \begin{cases} 1 - \frac{3}{2} \frac{T}{m} & T \ll m \\ \frac{m}{2T} & T \gg m \end{cases}$$

For these expressions, it is important to keep the $\mathcal{O}(1/x)$ in the asymptotic form of the Bessel functions for large x .

Appendix B: Entropy production

In the body of the text, we have used energy transfer from the HS to the VS to determine the evolution of T'/T from which we could get the entropy produced. One can also write equations directly giving the evolution of the entropy, as in [30]. Both approaches are equivalent, provided one takes into account the evolution of the effective degeneracy parameter of the VS. For simplicity, we assumed g_* constant during energy transfer for the analytical expressions but took into account its evolution for the numerical results. In this appendix, for the sake of comparison but also because of the specifics of our scenario, we derive some analytical expressions for entropy production, both for non-relativistic and relativistic decay. We use lower case letters for the entropy densities and upper case for comoving ones. Prime (unprime) quantities refer to the HS (resp. VS). Total quantities are written with a lower index t , e.g. $S_t = S' + S$ is the total comoving entropy, with $S_t = s_t a^3$.

1. Non-relativistic decay

To set the ground, we start with the standard case of entropy production through the decay of a NR particle that comes to dominate the expansion of the Universe [13, 30]. The heat transfer from decay satisfies

$$dQ = dE + pdV = -dQ' \quad (\text{B1})$$

as the pressure of the NR decaying particles can be neglected. The comoving entropy of the VS particles, all assumed to be relativistic, evolves as

$$\frac{dS}{dt} \equiv \frac{1}{T} \frac{dQ}{dt} = -\frac{1}{T} \frac{d(\rho' a^3)}{dt} \quad (\text{B2})$$

with $\rho' = m' n'$. Thus

$$\frac{dS}{dt} = \frac{\Gamma'}{T} \rho' a^3 \quad (\text{B3})$$

with

$$\rho' a^3 = \rho'_i a_i^3 e^{-\Gamma'(t-t_i)} \quad (\text{B4})$$

Using MB statistics, $S = 4g_* T^3 a^3 / \pi^2$ (appendix A), this can be written as

$$S^{1/3} \frac{dS}{dt} = \left(\frac{4g_*}{\pi^2} \right)^{1/3} \Gamma' \rho' a^4 \quad (\text{B5})$$

and

$$S^{4/3} = S_i^{4/3} + \frac{4}{3} \left(\frac{4}{\pi^2} \right)^{1/3} \Gamma' \rho'_i a_i^4 \int_{t_i}^t dt' g_*^{1/3} \frac{a}{a_i} e^{-\Gamma'(t'-t_i)} \quad (\text{B6})$$

Integrating this expression requires to know $a(t)$ and, possibly, the evolution of g_* which depends on the temperature of the VS, T . We assume that the VS particles are always in equilibrium. If g_* is constant, using $a \propto t^{2/3}$ for the early MD evolution, the entropy produced for $(t - t_i) \lesssim \tau' = 1/\Gamma'$ evolves as

$$\left(\frac{S}{S_i} \right)^{4/3} \approx 1 + \frac{3}{5} \frac{\rho'_i \Gamma'}{\rho_i H_i} \left(\left(\frac{t}{t_i} \right)^{5/3} - 1 \right) \quad (\text{B7})$$

where we have used MB statistics to express $s_i^{4/3}$ in terms of ρ_i .⁶ We see that $S \propto t^{5/4} \sim a^{15/8}$ for $a \propto t^{2/3}$ and thus $T \propto a^{-3/8}$ once the second term becomes dominant, see fig.1. Notice that entropy production at early times depends on the heating parameter which we introduced in the bulk of this article, $\kappa \sim (\rho'/\rho)(\Gamma'/H)$, see eq.(6). At late times, $t \gtrsim \tau'$, the entropy of the VS is

$$\left(\frac{S_f}{S_i} \right) \approx (\Gamma(5/3))^{3/4} \left(\frac{\rho'_i}{\rho_i} \right)^{3/4} \left(\frac{\tau'}{t_i} \right)^{1/2} \quad (\text{B8})$$

assuming $S_f \gg S_i$, with $\Gamma(5/3) \approx 0.9$. This is hardly new [13, 30]. Nevertheless, a couple of features are worth noticing for our problem.

First, we notice that, as the ratio of matter to radiation evolves $\rho_m/\rho_r \propto a$ which is $\sim t^{2/3}$ in a MD era, (B8) can be written in terms of the ratio of energy densities at τ' as if the particle had not decayed

$$\frac{S_f}{S_i} \approx \left(\frac{\rho'}{\rho} \right)_{\text{nodecay}}^{3/4} \quad (\text{B9})$$

Thus, the entropy produced is as if it had been stored in the decaying particle. Thus, the latter the decay, the larger is the entropy produced. The standard situation is the decay of massive particle that come to dominate the expansion at some $t_i = t_{\text{eq}}$ [13, 30]. At that moment, $\rho'_{\text{eq}} = \rho_{\text{eq}}$ and so the entropy produced is simply (and

⁶ Note that, for any statistics, $s^{4/3} \approx g^{1/3} \rho$ to within 1%, regardless of the statistics (MB, FD or BE), see appendix A.

quite nicely) given by

$$\frac{S_f}{S_{\text{eq}}} \approx \left(\frac{\tau'}{t_{\text{eq}}} \right)^{1/2} \quad (\text{B10})$$

In the bulk of this work, we consider a scenario in which a particle (a dark photon) becomes NR while it is driving the expansion of the universe. In that case, $t_i = t_{\text{nr}}$ and the entropy of the VS is related to that in the HS by $S_{\text{nr}} = (g_*/g'_*\xi^3)_{\text{nr}} S'_{\text{nr}} \ll S'_{\text{nr}}$ where $\xi = T'/T \gg 1$. Thus, in that situation, the total entropy produced is given by

$$\frac{S_{t,f}}{S_{t,i}} \approx \frac{S_f}{S'_i} \approx \left(\frac{g_*}{g'_*} \right)^{1/4} \left(\frac{\tau'}{t_{\text{nr}}} \right)^{1/2} \quad (\text{B11})$$

Alternatively, we can consider a scenario in which the particle is subdominant when it becomes NR but eventually dominates the Universe at t_{eq} before decaying. Between t_{nr} and t_{eq} , $\rho \propto a^{-4} \propto t^{-2}$ and $\rho' \propto a^{-3} \propto t^{-3/2}$, so that $t_{\text{nr}}/t_{\text{eq}} = (\rho'_{\text{nr}}/\rho_{\text{nr}})^2$. From (B10), the entropy produced reads

$$\frac{S_{t,f}}{S_{t,i}} \approx \frac{\rho'_{\text{nr}}}{\rho_{\text{nr}}} \left(\frac{\tau'}{t_{\text{nr}}} \right)^{1/2} \quad (\text{B12})$$

Finally, we can give the entropy produced if the massive particle is decaying when the expansion is RD, driven by the VS, a case which is relevant if $\xi \ll 1$. Replacing $a \propto t^{2/3}$ by $a \propto t^{1/2}$ in (B6) gives

$$\left(\frac{S_f}{S_i} \right)^{4/3} \approx 1 + \Gamma(3/2) \frac{\rho'_i}{\rho_i} \left(\frac{\tau'}{t_i} \right)^{1/2} \quad (\text{B13})$$

The second term can be expressed as the ratio of energy densities at decay assuming no entropy release, since $\rho_m/\rho_r \propto t^{1/2}$ in a RD era, and so is a small contribution as long as $\rho \gtrsim \rho'$.

2. Relativistic decay

Next we consider entropy production when both the HS and VS are made of relativistic particles, which do work when the volume is changing. The heat transfer satisfies

$$dQ = -dQ' \equiv -(dE' + p'dV) \quad (\text{B14})$$

with $p' = \rho'/3$ and so the rate of entropy increase of the VS is given by

$$\frac{dS}{dt} = -\frac{1}{aT} \frac{d(\rho'a^4)}{dt} \quad (\text{B15})$$

From section II, we can write this as

$$\frac{dS}{dt} = \frac{m'\Gamma'}{3T'T} \rho'a^3 \quad (\text{B16})$$

neglecting inverse decay. Notice that the entropy of the HS evolves as

$$\frac{dS'}{dt} = -\frac{m'\Gamma'}{3T'^2} \rho'a^3, \quad (\text{B17})$$

with no factor of $T \ll T'$, so the total entropy increases: $\dot{S}_t > 0$.

With $s = 4g_*T^3/\pi^2$ (MB!), we can rewrite (B16) as

$$S^{1/3} \frac{dS}{dt} = \left(\frac{4g_*}{\pi^2} \right)^{1/3} \frac{m'\Gamma'}{3T'} \rho'a^4 \quad (\text{B18})$$

This is the same expression as (B5), provided $\Gamma' \rightarrow m'\Gamma'/3T'$. This can be integrated analytically for all t , provided $g_* = \text{const}$ and $\rho' \gg \rho$. First, with $T' \propto 1/a$, we have

$$\rho' = \rho'_i \frac{a_i^4}{a} e^{-\frac{4m'\Gamma'}{9T'_i H_i} ((a/a_i)^3 - 1)}, \quad (\text{B19})$$

see Eq.(10). Next, using MB statistics to express s_i in terms of ρ_i , we get

$$\left(\frac{S}{S_i} \right)^{4/3} \approx 1 + \frac{1}{3} \frac{\rho'_i}{\rho_i} \left(1 - e^{-\frac{4m'\Gamma'}{9T'_i H_i} ((a/a_i)^{3/2} - 1)} \right) \quad (\text{B20})$$

At early times, entropy production depends on the heating parameter $\kappa_i = (\rho'_i/3\rho_i)\langle\Gamma'_i\rangle/H_i$ introduced in eq.(6),

$$\left(\frac{S}{S_i} \right)^{4/3} \approx 1 + \frac{8}{9} \kappa_i \left(\frac{a}{a_i} \right)^3 \quad (\text{B21})$$

taking $a \gg a_i$. It becomes significant only after contact, $\kappa_i \left(\frac{a}{a_i} \right)^3 \approx 1$ (see III A 2) and then grows slowly as $S \propto t^{9/8} \sim a^{9/4}$ as $a \propto t^{1/2}$, corresponding to a temperature of the VS that evolves $T \propto a^{-1/4}$, see fig.1. After thermalization, $\langle\Gamma'\rangle/H \gtrsim 1$, and

$$\left(\frac{S_f}{S_i} \right) \approx \left(\frac{\rho'_i}{\rho_i} \right)^{3/4} \rightarrow \frac{S_{t,f}}{S_{t,i}} \approx \frac{S_f}{S'_i} \approx \left(\frac{g_*}{g'_*} \right)^{1/4} \quad (\text{B22})$$

This means that the energy from the HS has been transferred to the VS, $g_*T_f^4 a_f^4 \approx g'_*T_i^4 a_i^4$ assuming $g_* \gg g'_*$ [31]. Unlike the case of decay of a non-relativistic particle, the entropy produced is independent of the decay rate, see eq.(B11). Matching with (B22) is obtained by setting $t_{\text{nr}} \approx \tau'$, corresponding to a HS particle that would become non-relativistic right at the time of thermalization. The entropy production in the process of energy transfer between the two RD sectors is quite mild,

$S_f/S'_i \approx 2.4$ for $g'_* = 3$ and $g_* \approx 100$. This is to be contrasted to the decay of a NR particle, in which case the entropy produced grows with the particle lifetime. This is essentially due to the fact that $\rho'/\rho \propto a$ for NR particles in the HS while it is constant for relativistic particles, see eq.(B9).

Appendix C: Boltzmann equations

In this appendix, we address some technical aspects associated with the three Boltzmann equations that govern the coupled HS-VS system, Eqs.(3), (4) and (5). The first of these is the continuity equation and is well known. The second comes from the standard Boltzmann equation for number density considering only decay and inverse decay, $\gamma' \leftrightarrow f\bar{f}$, but must be modified to account for the different temperatures of the sectors. We have

$$\frac{dn'}{dt} + 3Hn' = \int d\Pi_1 d\Pi_2 d\Pi' |\mathcal{M}|^2 (2\pi)^4 \delta^4(p_1 + p_2 - p') \times (f_1 f_2 - f'). \quad (\text{C1})$$

We assume that the SM fermions have equilibrium MB distributions, $f_1 f_2 = e^{-(E_1 + E_2)/T}$, while we allow for a possible dark photon chemical potential by taking $f' = e^{(\mu' - E')/T'}$ (note that f' should have the shape of an equilibrium distribution, since the dark photons were initially equilibrated). Integrating this, one can recover eq.(4). This expression can also be written as

$$\frac{dn'}{dt} + 3Hn' = \langle \Gamma' \rangle_T n_{\text{eq}}(T) - \langle \Gamma' \rangle_{T'} n'(T') \quad (\text{C2})$$

where the angled brackets denote thermal averaging,

$$\langle \Gamma' \rangle_T = \Gamma' \frac{K_1(m'/T)}{K_2(m'/T)}. \quad (\text{C3})$$

The continuity equation, given in eq.(3), describes how the total energy density in the Universe changes over time. The total equation of state is

$$w_{\text{tot}} = \frac{p + p'}{\rho + \rho'} = w' \frac{\rho'}{\rho_{\text{tot}}} + \frac{\rho_{\text{tot}} - \rho'}{3\rho_{\text{tot}}}, \quad (\text{C4})$$

using $w = 1/3$, since we are always concerned with times where the SM is radiation-dominated.

Finally, the equation for energy transfer, eq.(5), can be derived similarly, starting with

$$\frac{d\rho'}{dt} + 3(1 + w')H\rho' = \int d\Pi_1 d\Pi_2 d\Pi' |\mathcal{M}|^2 (2\pi)^4 \times \delta^4(p_1 + p_2 - p') (f_1 f_2 - f') E', \quad (\text{C5})$$

using the same distribution functions and integrating.

Eqs.(3), (4) and (5) give three coupled differential

equations for ρ , ρ' and n' . We solve them as a function of the scale factor, a , rather than of time, t , by using $d/dt = (aH)d/da$. This is different from the standard procedure, in which these equations are solved in terms of some m/T . When the dark photon is relativistic, one can change variables by using $T'da = -adT'$, and similarly when it is non-relativistic we have $2T'da = -adT'$. However, the relation between a and T' at intermediate times is more involved, particularly since there may also be entropy production at the same time.

Keeping our equations in a , we must express several different quantities in terms of the scale factor. The equation of state in the visible sector is always $w = 1/3$, while in the hidden sector it turns out to be well-approximated at all times by

$$w' \simeq \frac{1}{3} \left[1 - \left(\frac{m'n'}{\rho'} \right)^2 \right]. \quad (\text{C6})$$

Then the usual dimensionless quantity $x' \equiv m'/T'$, which enters explicitly in eq.(4), is found by

$$x' = \frac{m'n'}{p'} = \frac{m'n'}{w'\rho'} \quad (\text{C7})$$

Appendix D: Comments on numerical solutions

In the body of the text, we focused on approximate analytical solutions and their comparison to the numerical solutions depicted in fig.3. Here we add some brief comments on our numerical resolution of eqs.(3-5). We solve for ρ' , n' and ρ and define from these quantities the temperature T of the VS, a proxy for the same quantity T' for the HS and finally the chemical potential μ' . Other quantities, like entropy densities, are obtained using standard but general equilibrium relations, eg $s' = (\rho' + p' - \mu'n')/T'$. For $T' \hat{=} \langle E' \rangle / 3$ (MB), we found convenient to define it through $T' = p'/n' = w'\rho'/n'$, where the HS equation of state, $p' = w'\rho'$, is approximated by (C6), a simple function that smoothly interpolates between the relativistic and non-relativistic regimes of the dark photons. As the system evolves, the dark photons can develop a non-zero chemical potential μ' , which can be read out from n' or ρ' once T' is determined. This is the case when the dark photons become non-relativistic as they are free streaming, and so, more abundant than their thermal equilibrium value. In that case, the temperature evolves as $T' \approx 1/a^2$ and their chemical potential as $\mu' - m' \propto T'/T'_{\text{nr}}$ [13].

A non-zero chemical potential can also arise for relativistic dark photons. This is in particular the case when the HS and the VS approach thermalization. This is related to the bumpy features around ξ approaches 1 that are visible in the numerical solutions in fig. 3. To gain some understanding of the origin of these features, we combine Eqs.(4) and (5). Neglecting the inverse process

and using $K_1(x')/K_2(x') \approx x'/2$ and $\rho'/n' \approx 3T'$ gives the following equation for T' ,

$$\frac{dT'}{da} + \frac{T'}{a} \approx \frac{\Gamma'}{3Ha} \left(\frac{\rho'x'}{2n'} - m' \right) \approx \frac{\Gamma'm'}{6Ha} \quad (\text{D1})$$

Notice that the that rhs is positive. As long as $\langle \Gamma' \rangle / H \ll 1$, this term can be neglected and the temperature evolves as $T' \propto a^{-1}$, corresponding to the attractor evolution, see section III A 2. Eventually, the rhs becomes significant, $\langle \Gamma' \rangle / H \sim 1$, and so T' decreases more slowly than a^{-1} , leading to a levering of $\xi = T'/T$ close to thermalization and so to the bumpy feature visible for instance in the lower left panel of fig.3. This is due to time dilation, which at late time leads to a depletion of the γ' particle distribution at low energies and so, effectively, to an increase of their mean energy $\sim T'$. This transient period does not last long, as T'/T approaches 1 exponentially fast at the time of thermalization, introducing a slight delay in the thermalization process if $g_* \gg g'_*$, see section III A 3. A more detailed but preliminary analysis, based of the evolution of the γ' particle distribution, is in progress [73]; it basically supports the validity of the above assertions.

Appendix E: Freeze-in and thermalization of dark photons

In this appendix, we consider the case $\xi_i \ll 1$. So we assume that the expansion is radiation dominated and driven by the VS, $T \gg T'$ and consider freeze-in production of dark photons and their subsequent decay. We do so to assess the possible impact of FI on the initial temperature ratio, $\xi_i \ll 1$. If $T \gg T'$, it is in principle required to take into account modifications of the ordinary photon propagation modes due to thermal corrections to accurately track the freeze-in production of dark photons [34, 35, 74]. Nevertheless, as the final abundance of dark photons is dominated by the inverse decay process [35, 44], to simplify our discussion, in this brief appendix we neglect these subtleties and just take into account inverse decay to estimate the late abundance of dark photons.⁷

The expansion is RD and driven by the VS if $\xi_i \ll 1$ but also more generally when $\rho' \ll \rho$ along the evolution of the coupled VS and HS. In particular, this is the case both after relativistic thermalization or when the dark photons are non-relativistic but already decaying, $t \gtrsim \tau'$, so that their abundance is exponentially suppressed. In

all these cases, we may rewrite the equation (4) for the abundance of DP as

$$\frac{dY'}{dt} + \sigma' x Y' \approx \frac{g'}{8g_*} \sigma' x^3 K_1(x) \quad (\text{E1})$$

where $x = m'/T$, $Y' = n'/s$ and $\sigma' = \Gamma'/H' \lesssim 1$ with $H' = H(m')$. The lhs takes into account dark photon decay while the rhs is the source terms from FI production. As before in the present work, we have used MB statistic to express n'_{eq} and $\langle \Gamma' \rangle$ in terms of Bessel functions, cf appendix A. This Boltzmann equation is readily integrated to give

$$Y' = Y'_i e^{-\frac{\sigma'}{2}(x^2 - x_i^2)} + \frac{g'}{8g_*} \sigma' \int_{x_i}^x dx' x'^3 K_1(x') e^{-\frac{\sigma'}{2}(x^2 - x'^2)} \quad (\text{E2})$$

The first term on rhs represents the decay of the initial dark photon abundance, $e^{-\sigma' x^2/2} \sim e^{-t/\tau'}$; the second one represents their production from the VS convoluted by dark photon decay.

The simple expression (E2) captures several features that we observed in the more complicated problem of reheating of the VS from a HS. For the sake of brevity, we just sketch the key results, which can be readily verified by inspection of the general solution. For this, we refer to figure 7 in which some typical solutions are depicted.

Consider first the solid lines, say for $\xi_i = 10^{-3}$. The abundance is initially characterized by a plateau $Y' \approx Y'_i \propto \xi_i^3$, analogous to the plateau in the case of a hot HS. For such choice of parameters, the initial temperature ratio is stable and we can discuss the freeze-out of DM along the line of section V, with $\xi_{\text{fo}} = \xi_i$. Eventually, freeze-in production of dark photons becomes relevant. This occurs essentially when the heating parameter $\kappa' \sim (1/Y') \langle \Gamma' \rangle / H$ becomes $\mathcal{O}(1)$, marking the onset of dark photon creation from the VS, after which $Y' \propto a^3$ (and so $\xi \propto a$). This combination of parameters is akin to the heating parameter $\kappa \sim (\rho'/\rho) \langle \Gamma' \rangle / H$ in the problem of heating of the VS from the HS.⁸ Different choices of ξ_i depict the same behaviour and for all they track the production of dark photons, a curve which in that respect behaves as an attractor. Such behavior includes cases in which ξ_i is very low. For instance, for $\xi_i = 10^{-6}$, the abundance of dark photons produced by freeze-in increases rapidly (see solid purple line) toward this attractor solution. This sharp initial increase of the number of

⁷ If $T' \gg T$, we deem that thermal effects are negligible in the process of reheating of the VS. First, the dark photons are essentially non-interacting. Second the VS is much colder than the HS so that the impact of thermal corrections, such as modification of the mass of the SM degrees of freedom is a small disturbance to the process of reheating of the VS.

⁸ There is slight difference between the criteria for the onset of particle creation $\sim (1/Y') \langle \Gamma' \rangle / H \sim 1$ and that of energy transfer $\kappa' \sim \rho/\rho' \langle \Gamma' \rangle / H \sim 1$ (heating parameter). For freeze-in, we deem more relevant to focus on the number density of dark photons rather than on their mean energy. For the problem of reheating of the VS, the key issue is of course that of energy transfer.

dark photons is analogous to the rapid increase of temperature to T_{\max} in the problem of reheating of the VS. This occurs when $\kappa' \sim (1/Y_i)\langle\Gamma'\rangle_i/H'_i \gtrsim 1$ at the initial moment. In that case, the initial choice of ξ_i is unstable. In the body of the text and in figure 6 we require that

$$\kappa'_i \approx \frac{\rho_i}{3\rho'_i} \frac{\langle\Gamma'\rangle_i}{H'_i} \lesssim 1 \quad (\text{E3})$$

for the stability of the initial temperature ratio when $\xi_i \lesssim 1$, see section V B.

After freeze-in production, the dark photons are non-relativistic and $Y' \sim \text{constant}$ until decay becomes relevant. As the solid and dotted curves show, the largest the freeze-in production, the earlier the decay of the dark photons. That trivially results from the fact that their creation and disappearance are controlled by related processes (inverse and direct decay), in other words by the kinetic mixing parameter. In particular, a dark photon that would reach $Y' \sim Y'_{\text{eq}}$ at $T \sim m$ would, by definition, be in thermal equilibrium and would subsequently track their equilibrium abundance, $n' \propto e^{-m'/T}$, see the dot-dashed curve in fig. 7. For a smaller kinetic mixing, their abundance will overshoot the equilibrium abundance until they start to decay, $n' \propto e^{-\Gamma't}$, see solid and dotted curves. As is known since some time, see [38], such dark photons may eventually thermalize with the VS if $n' \propto e^{-\Gamma't} \sim n'_{\text{eq}}(T)$, see solid curves and their merging with the equilibrium abundance. Such outcome is of course only relevant if the number density n' is not a ridiculously small number when that condition is met,

see short dashed curve.

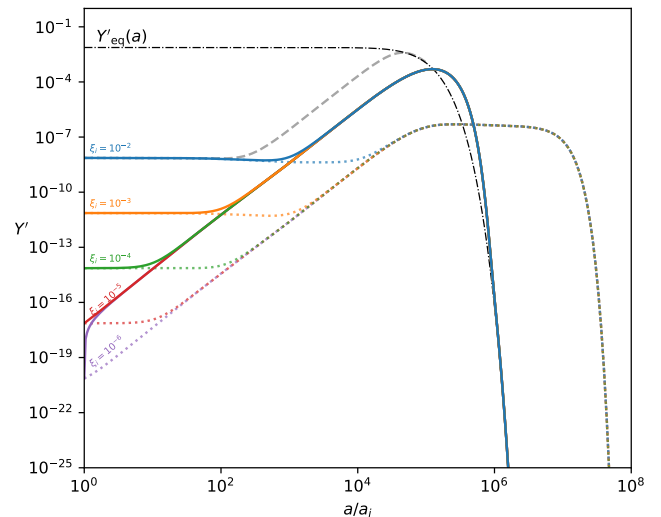


Figure 7: Examples of evolution of dark photons abundance for $\xi_i \ll 1$. The mass m' is fixed at 5 MeV. The solid curves correspond to a value for ε of $10^{-9.4}$, only differing by the value of ξ_i , and the long-dashed one to an $\varepsilon = 10^{-8.5}$. The dotted curves are obtained by setting ε to 10^{-11} . One can observe the attractor behavior for the curves that share the same ε and, afterwards, the contact point between Y' and its equilibrium value Y'_{eq} for this choice of parameters.

-
- [1] B. Patt and F. Wilczek (2006), hep-ph/0605188.
[2] R. Foot, H. Lew, and R. R. Volkas, Phys. Lett. B **272**, 67 (1991).
[3] M. J. Strassler and K. M. Zurek, Phys. Lett. B **651**, 374 (2007), hep-ph/0604261.
[4] D. Curtin and R. Sundrum (2017), 1702.02524.
[5] D. N. Spergel and P. J. Steinhardt, Phys. Rev. Lett. **84**, 3760 (2000), astro-ph/9909386.
[6] S. Tulin and H.-B. Yu, Phys. Rept. **730**, 1 (2018), 1705.02358.
[7] P. Schwaller, Phys. Rev. Lett. **115**, 181101 (2015), 1504.07263.
[8] S. Dodelson and L. M. Widrow, Phys. Rev. Lett. **72**, 17 (1994), hep-ph/9303287.
[9] J. McDonald, Phys. Rev. Lett. **88**, 091304 (2002), hep-ph/0106249.
[10] L. J. Hall, K. Jedamzik, J. March-Russell, and S. M. West, JHEP **03**, 080 (2010), 0911.1120.
[11] X. Chu, T. Hambye, and M. H. G. Tytgat, JCAP **05**, 034 (2012), 1112.0493.
[12] N. Bernal, M. Heikinheimo, T. Tenkanen, K. Tuominen, and V. Vaskonen, Int. J. Mod. Phys. A **32**, 1730023 (2017), 1706.07442.
[13] E. W. Kolb and M. S. Turner, *The Early Universe*, vol. 69 (1990), ISBN 978-0-201-62674-2.
[14] A. Berlin, D. Hooper, and G. Krnjaic, Phys. Lett. B **760**, 106 (2016), 1602.08490.
[15] L. Heurtier and F. Huang, Phys. Rev. D **100**, 043507 (2019), 1905.05191.
[16] F. Ertas, F. Kahlhoefer, and C. Tassilo, JCAP **02**, 014 (2022), 2109.06208.
[17] R. Garani, M. Redi, and A. Tesi, JHEP **12**, 139 (2021), 2105.03429.
[18] Z. G. Berezhiani, A. D. Dolgov, and R. N. Mohapatra, Phys. Lett. B **375**, 26 (1996), hep-ph/9511221.
[19] P. Adshead, Y. Cui, and J. Shelton, JHEP **06**, 016 (2016), 1604.02458.
[20] E. Hardy and J. Unwin, JHEP **09**, 113 (2017), 1703.07642.
[21] T. Tenkanen and V. Vaskonen, Phys. Rev. D **94**, 083516 (2016), 1606.00192.
[22] P. Sandick, B. S. Es Haghi, and K. Sinha, Phys. Rev. D **104**, 083523 (2021), 2108.08329.
[23] A. Ireland and S. Koren (2022), 2211.13212.
[24] M. Pospelov, A. Ritz, and M. B. Voloshin, Phys. Lett. B **662**, 53 (2008), 0711.4866.
[25] S. Hannestad and J. Madsen, Phys. Rev. D **52**, 1764 (1995), astro-ph/9506015.
[26] M. Kawasaki, K. Kohri, and N. Sugiyama, Phys. Rev. D **62**, 023506 (2000), astro-ph/0002127.

- [27] L. Ackerman, M. R. Buckley, S. M. Carroll, and M. Kamionkowski, *Phys. Rev. D* **79**, 023519 (2009), 0810.5126.
- [28] J. L. Feng, M. Kaplinghat, H. Tu, and H.-B. Yu, *JCAP* **07**, 004 (2009), 0905.3039.
- [29] B. Holdom, *Phys. Lett. B* **166**, 196 (1986).
- [30] R. J. Scherrer and M. S. Turner, *Phys. Rev. D* **31**, 681 (1985).
- [31] R. Coy, T. Hambye, M. H. G. Tytgat, and L. Vanderheyden, *Phys. Rev. D* **104**, 055021 (2021), 2105.01263.
- [32] K. Griest and M. Kamionkowski, *Phys. Rev. Lett.* **64**, 615 (1990).
- [33] N. Bernal, P. Konar, and S. Show (2023), 2311.01587.
- [34] H. An, M. Pospelov, and J. Pradler, *Phys. Lett. B* **725**, 190 (2013), 1302.3884.
- [35] T. Hambye, M. H. G. Tytgat, J. Vandecasteele, and L. Vanderheyden, *Phys. Rev. D* **100**, 095018 (2019), 1908.09864.
- [36] A. Arvanitaki, S. Dimopoulos, M. Galanis, D. Racco, O. Simon, and J. O. Thompson, *JHEP* **11**, 106 (2021), 2108.04823.
- [37] M. Fairbairn, E. Hardy, and A. Wickens, *JHEP* **07**, 044 (2019), 1901.11038.
- [38] J. A. Harvey, E. W. Kolb, D. B. Reiss, and S. Wolfram, *Nucl. Phys. B* **201**, 16 (1982).
- [39] S. Hannestad, *Phys. Rev. D* **70**, 043506 (2004), astro-ph/0403291.
- [40] S. Dodelson and M. S. Turner, *Phys. Rev. D* **46**, 3372 (1992).
- [41] G. Mangano, G. Miele, S. Pastor, T. Pinto, O. Pisanti, and P. D. Serpico, *Nucl. Phys. B* **729**, 221 (2005), hep-ph/0506164.
- [42] A. Berlin, D. Hooper, and G. Krnjaic, *Phys. Rev. D* **94**, 095019 (2016), 1609.02555.
- [43] P. Gondolo and G. Gelmini, *Nucl. Phys. B* **360**, 145 (1991).
- [44] J. Berger, K. Jedamzik, and D. G. E. Walker, *JCAP* **11**, 032 (2016), 1605.07195.
- [45] G. F. Giudice, A. Riotto, and I. Tkachev, *JHEP* **11**, 036 (1999), hep-ph/9911302.
- [46] C. Mondino, M. Pospelov, J. T. Ruderman, and O. Slone, *Phys. Rev. D* **103**, 035027 (2021), 2005.02397.
- [47] T. Bringmann, P. F. Depta, M. Hufnagel, and K. Schmidt-Hoberg, *Phys. Lett. B* **817**, 136341 (2021), 2007.03696.
- [48] M. Bauer, P. Foldenauer, and J. Jaeckel, *JHEP* **07**, 094 (2018), 1803.05466.
- [49] E. Hardy and R. Lasenby, *JHEP* **02**, 033 (2017), 1611.05852.
- [50] G. Arcadi, O. Lebedev, S. Pokorski, and T. Toma, *JHEP* **08**, 050 (2019), 1906.07659.
- [51] M. Hufnagel, K. Schmidt-Hoberg, and S. Wild, *JCAP* **02**, 044 (2018), 1712.03972.
- [52] M. Hufnagel, Ph.D. thesis, Hamburg U., Hamburg (2020).
- [53] J. D. Bjorken, S. Ecklund, W. R. Nelson, A. Abashian, C. Church, B. Lu, L. W. Mo, T. A. Nunamaker, and P. Rassmann, *Phys. Rev. D* **38**, 3375 (1988).
- [54] C. Athanassopoulos et al. (LSND), *Phys. Rev. C* **58**, 2489 (1998), nucl-ex/9706006.
- [55] F. Bergsma et al. (CHARM), *Phys. Lett. B* **166**, 473 (1986).
- [56] J. Blumlein et al., *Z. Phys. C* **51**, 341 (1991).
- [57] J. Blümlein and J. Brunner, *Phys. Lett. B* **731**, 320 (2014), 1311.3870.
- [58] S. Alekhin et al., *Rept. Prog. Phys.* **79**, 124201 (2016), 1504.04855.
- [59] I. Baldes and K. Petraki, *JCAP* **09**, 028 (2017), 1703.00478.
- [60] M. M. Flores and K. Petraki (2024), 2405.02222.
- [61] T. Hambye, M. Lucca, and L. Vanderheyden, *Phys. Lett. B* **807**, 135553 (2020), 2003.04936.
- [62] M. Hufnagel and M. H. G. Tytgat (2022), 2212.09759.
- [63] P. A. Zyla et al. (Particle Data Group), *PTEP* **2020**, 083C01 (2020).
- [64] S. Davidson, E. Nardi, and Y. Nir, *Phys. Rept.* **466**, 105 (2008), 0802.2962.
- [65] D. E. Morrissey and M. J. Ramsey-Musolf, *New J. Phys.* **14**, 125003 (2012), 1206.2942.
- [66] M. Dine and A. Kusenko, *Rev. Mod. Phys.* **76**, 1 (2003), hep-ph/0303065.
- [67] G. Elor, M. Escudero, and A. Nelson, *Phys. Rev. D* **99**, 035031 (2019), 1810.00880.
- [68] K. D. Lozanov (2019), 1907.04402.
- [69] S. Davidson, M. Losada, and A. Riotto, *Phys. Rev. Lett.* **84**, 4284 (2000), hep-ph/0001301.
- [70] K. Kajantie, M. Laine, K. Rummukainen, and M. E. Shaposhnikov, *Phys. Rev. Lett.* **77**, 2887 (1996), hep-ph/9605288.
- [71] P. B. Arnold, D. Son, and L. G. Yaffe, *Phys. Rev. D* **55**, 6264 (1997), hep-ph/9609481.
- [72] S. Clery and J. Kimus (2024), 24XX.YYYYY.
- [73] M. Hufnagel, J. Kimus, and M. H. G. Tytgat (in progress).
- [74] C. Dvorkin, T. Lin, and K. Schutz, *Phys. Rev. D* **99**, 115009 (2019), [Erratum: *Phys.Rev.D* 105, 119901 (2022)], 1902.08623.